Summer 2010

Organization of Human Sperm Chromosomes During Pronuclei Formation

Estella Jones
Old Dominion University

ORGANIZATION OF HUMAN SPERM CHROMOSOMES DURING PRONUCLEI FORMATION

by

Estella Jones
B.A. 1992, Virginia Wesleyan College
M.S. 1999, Eastern Virginia Medical School

A Dissertation Submitted to the Faculty of
Eastern Virginia Medical School and Old Dominion University
in Partial Fulfillment of the
Requirement for the Degree of

DOCTOR OF PHILOSOPHY

BIOMEDICAL SCIENCES

EASTERN VIRGINIA MEDICAL SCHOOL
And OLD DOMINION UNIVERSITY
August 2010

Approved by:

Andrei Zalensky (Director)

Sergio Oehninger (Member)

Silvina Bocca (Member)

Jacob Mayer (Member)

Peter Sutovsky (Member)

ABSTRACT

ORGANIZATION OF HUMAN SPERM CHROMOSOMES DURING PRONUCLEI FORMATION

Estella Jones
Eastern Virginia Medical School and
Old Dominion University, 2010
Director: Dr. Andrei Zalensky

Chromosome organization is regarded as an important factor in regulating gene expression. In addition to the histone code, it is a part of the epigenetic mechanisms participating in fertilization and early embryonic development. Recent studies have demonstrated that chromosomes of human spermatozoa have well-defined spatial organization that includes preferred intranuclear positioning. The hypothesis of this dissertation is that sperm chromosome architecture participates in controlled transformation and activation of the paternal genome following fertilization.

Adequate model systems are necessary to study early nuclear events characteristic of human fertilization. This research focused on introduction and application of heterologous intracytoplasmic sperm injection (ICSI) to study sperm chromosomes remodeling in ooplasm. ICSI of human sperm into bovine and hamster oocytes was explored in detail and the latter pair has been chosen for further studies as robust and apparently faithful models of the paternal gamete development.

In this work, it was established that after ICSI: 1) sperm cells with partially digested membranes and depleted of acrosome decondense more rapidly and to a greater extent than intact cells; and 2) marked sperm-to-sperm variability in degree of chromatin swelling exists during all stages of pronuclear development as detected by DNA staining

in zygotes. The latter characteristic is proposed to reflect the cryptic nuclear heterogeneity in population of morphologically, mature normal sperm.

Chromatin transformation in pronuclei was established by immunolocalizaton of protamines in zygotes. Protamine withdrawal is rapid (completed within 1 hr) and correlates with pronuclear area rather than with specific time post ICSI. We propose that such behavior is again a consequence of hidden variability in sperm population.

The final part involved the post fertilization study of two human sperm chromosomes – Homo Sapiens (HSA) chromosomes 18 and 19. Findings demonstrated that in sperm: 1) both chromosomes are packed into compact territories; and 2) similar to somatic cells, gene-rich HSA19 is positioned internally while gene-poor HSA18 peripherally. The unwinding of HSA18/19 in developing pronuclei was described. To visualize structure remodeling of sperm chromosomes in zygotes, novel FISH procedures were developed.

These findings suggest that remodeling of human sperm in heterologous ICSI faithfully mimics early steps of natural human fertilization and for the first time demonstrated several novel aspects of nuclear and chromosome reorganization during male pronuclei development.

This dissertation is dedicated to my mother, Nora Jones. Without her unconditional love, and unselfish support, I would not have been here today. Nobody could ask for a better mother than you.

I also dedicate this dissertation to my sister, Kathy Jones Burchett, her husband Danny, and my two nephews, Gage and Hunter. Their love and commitment through out this endeavor have enabled me to achieve this goal.

Last but not least, I would love to dedicate this to my beloved father, Frank Jones, who will not be able to witness this triumph but always knew I could do it. He was my biggest fan. I miss you Dad.

ACKNOWLEDGMENTS

There are many people who have contributed to the successful completion of this dissertation. I would like to thank the members of my dissertation committee, Dr. Oehninger, Dr. Bocca, Dr. Mayer, and Dr. Sutovsky for their patience and guidance on my research. My special thanks go to Dr. Godfrey and Leah Solomon who always gave the best advice to keep me on track throughout my doctoral training. I would like to thank my co-workers, Mrs. Donna Dowling-Lacey and Dr. Ting-Fung Chi for their warm friendship, dedication and steady support which helped me through the good times and bad times. I would also like to thank Dr. Irina Zalenskaya, Dr. Olga Mudrak, Dr. Igor Nazarov and Conrado Avendano for all of their patience, friendship and help in the research lab. In addition, I would like to thank Irene Foy, Diana Greene, Audra Mitchell, Victoria Kelley and Theresa Joseph for all the help and support they provided me over the course of this dissertation. I would like to thank my husband, Jonathan Currey, who has been completely supportive, understanding, encouraging and completely inspirational and always told me what a genius I was. Last but not least, I would like to thank Linda C. Hayhurst for the years and years and years of continued support and friendship and for putting up will all my stressed out rants--thanks for always being there.

The untiring efforts of my mentor and chair of my dissertation committee, Dr. Andrei Zalenksy, deserve special recognition. During these years, he has constantly supported, guided, and encouraged me. I could not have done it without him.

This work was funded by a grant from The Jones Foundation and, in part, by a National Institutes of Health grant (HD-042748) to AZ.

TABLE OF CONTENTS

Page

LIST OF TABLES viii

LIST OF FIGURES ix

LIST OF ABBREVIATIONS xi

Chapter

I. INTRODUCTION 1
- INTRODUCTION AND SPECIFIC AIMS 1
- INTRODUCTION TO SPERM NUCLEAR BIOLOGY AND PATERNAL CHROMATIN REMODELING 5
- PRELIMINARY RESULTS 14

II. DEVELOPMENT OF HETEROLOGOUS ICSI MODEL TO STUDY SPERM CHROMOSOME ORGANIZATION 18
- INTRODUCTION 18
- MATERIALS AND METHODS 20
- RESULTS 26
- DISCUSSION 29

III. KINETICS OF HUMAN MALE PRONUCLEAR DEVELOPMENT IN HETEROLOGOUS ICSI MODEL 32
- INTRODUCTION 32
- MATERIALS AND METHODS 33
- RESULTS 36
- DISCUSSION 40

IV. PROTAMINE WITHDRAWAL FROM HUMAN SPERM NUCLEI FOLLOWING HETEROLOGOUS ICSI INTO HAMSTER OOCYTES 44
- INTRODUCTION 44
- MATERIALS AND METHODS 46
- RESULTS 48
- DISCUSSION 52

V. INTRANUCLEAR POSITIONING OF HUMAN SPERM CHROMOSOMES 18 AND 19 56
- INTRODUCTION 56
- MATERIALS AND METHODS 58
- RESULTS 61
- DISCUSSION 64

VI. VISUALIZATION OF HUMAN SPERM CHROMOSOMES IN ZYGOTES FROM HETEROLOGOUS ICSI MODEL 67
INTRODUCTION.....67
MATERIALS AND METHODS 68
RESULTS.....70
DISCUSSION.....73

VII. SUMMARY 75

REFERENCES 78

VITA.....93

LIST OF TABLES

Table Page

1. Zygote nuclear changes in different treatment groups after ICSI of bovine oocytes with human perm.....30

2. Male pronuclear area of acrosome depleted (TX treated) and acrosome intact (control) sperm at different time points post heterologous ICSI..... 38

LIST OF FIGURES

Figure Page

1. Model of chromosome organization in human sperm.....10
2. Levels of chromosome organization in sperm head based on FISH data..... 11
3. Summary of sperm chromatin remodeling in mammals.....13
4. FISH visualization of sperm chromosomes.....15
5. Transformations of human sperm nuclei in Xenopus egg extracts.....16
6. Micromanipulator set-up for heterologous ICSI.....23
7. Typical result of HO-Hsp heterologous ICSI 16hr post ICSI.....26
8. Typical result of BO-Hsp heterologous ICSI.....27
9. Typical result of BO-Hsp heterologous ICSI using DTT-treated sperm + ETOH activation 4hr post ICSI.....28
10. Typical result of BO-Hsp heterologous ICSI using pretreated sperm (0.5 mM DTT + ionophore) and ionophore egg activation 3x10 min post ICSI.....28
11. Typical result of BO-Hsp heterologous ICSI using pretreated sperm (0.5 mM DTT + lysolecitin) with ionophore egg activation 3x10 min post ICSI.....29
12. Acrosomal status of human sperm as revealed by PNA staining.....36
13. Transformations of human sperm nuclei in hamster oocytes following heterologous ICSI.....37
14. Frequency distribution of mean mPN area demonstrates heterogeneity of sperm population.....39
15. Visualization of P1 and P2 in human sperm.....49
16. Dissociation of PRM from human sperm nuclei following heterologous (human sperm-hamster oocytes) ICSI.....51
17. Schematic representation of measurements used to determine (x,y) of CT centers (chromosome positioning).....60

18. Representative picture of FISH.....61

19. Intranuclear positioning of HSA 18 in human spermatozoa.....62

20. Intranuclear positioning of HSA 19 in human spermatozoa.....63

21. Unpacking of the sperm chromosome territory in zygotes.....71

22. Simultaneous imaging of two human chromosomes in zygotes.....72

LIST OF ABBREVIATIONS

3-D	Three dimensional
A23187	Calcium ionophore
AD	Acrosome depleted
AI	Acrosome Intact
BO	Bovine oocytes
BSA	Bovine serum albumin
CEN	centromere
CHR	Chromosome
CT	Chromosome territory
DAPI	4-, 6-diamidino-2-phenylindole
DTT	Dithiothreitol
ETOH	Ethanol
FA	Formamide
FISH	Fluorescent in situ hybridization
FITC-PNA	Fluorescent (FITC) labeled peanut agglutinin
HO	Hamster oocytes
HSA	Homo sapiens chromosome
Hsp	Human sperm
HTF	Human tubal fluid
Hup	Human protamine

ICSI	Intracytoplasmic sperm injection
MeOH	Methanol
mHTF	Modified human tubal fluid
mPN	Male pronucleus
NA	Nuclei areas
PI	Propidium iodide
PN	Pronucleus
PRM	Protamine
PVP	Polyvinyl pyrolidone
RT	Room temperature
SNBP	Sperm nuclear basic proteins
SSS	Synthetic serum substitute
TEL	Telomere
TR	Texas Red
TX	Trition X-100
XEE	*Xenopus Laevis* eggs extracts

CHAPTER I

INTRODUCTION

INTRODUCTION AND SPECIFIC AIMS

Chromosome (CHR) organization is regarded as an important factor in gene expression. In addition to DNA sequence level and histone code, it is an integrated part of the epigenetic mechanisms which play a major role in fertilization and early embryonic development. Nonetheless, CHR topology in gametes and zygotes is poorly studied. The long-term goal of this research is to establish the functional importance of human sperm genome architecture (configuration and the spatial arrangement of CHRs) in formation of pronuclei (PN) and early embryonic development. Human experiments are impossible due to ethical, legal and technical reasons; therefore reorganization of human sperm CHRs was studied with heterologous fertilization systems that model early events of natural fertilization. This dissertation is a part of a cooperative attempt to understand the role of sperm CHR positioning, modes of their withdrawal, structural reorganization, and movement during male pronuclear (mPN) formation and development. The **general hypothesis** is that unique genome architecture of sperm participates in the regulation of male genome activation during fertilization. The ultimate **goal** is to develop an experimental system, which allows accessing CHR function of fertile and infertile males involved in formation of an embryo.

The model journal for this dissertation is *Reproduction*.

The specific aims of this dissertation were to:

1. Develop a heterologous intracytoplasmic sperm injection (ICSI) approach to investigate transformation of human paternal genome at fertilization. In this aim, mPN development in the heterologous ICSI model using hamster and bovine oocytes injected with human sperm (Hsp) was studied. Intact and pretreated sperm were used along with various schemes of oocyte activation. The working hypothesis was that interspecies ICSI using hamster and/or bovine eggs and Hsp might provide relevant models to understand the early events of human fertilization. The goal was to choose optimal oocyte system and conditions of ICSI/zygote development.

2. Compare kinetics and patterns of mPN development in human/hamster ICSI using acrosome intact and acrosome depleted sperm cells. In Aim 1, an optimal heterologous ICSI system, based on hamster ova, was chosen to investigate the transformation of human paternal genome at fertilization. Here, the kinetics of mPN development at different time points post ICSI utilizing acrosome intact and acrosome depleted sperm were analyzed. During natural fertilization, the sperm acrosome, containing hydrolyzing enzymes, is shed as a result of the acrosome reaction. Thus, the acrosome and all its contents never enter the oocyte. In the ICSI procedure, the entire acrosome and its contents enter the ooplasm and cover the apical part of the sperm nuclei. The working hypothesis was that acrosome depleted sperm would yield more extensive pronuclear development in this heterologous ICSI model.

3. Characterize human protamines (PRMs) removal in hamster oocytes following ICSI. At fertilization, after the mature spermatozoa penetrate the oocyte, sperm chromatin is remodeled "back" from nucleoprotamine to nucleohistone state. While being crucial for

activation of male genome and ultimately for initiation of embryonic development, this process has not been studied in humans. In this Aim, the time frame post fertilization during which PRMs are withdrawn from the sperm nucleus was explored.

4. Determine intranuclear positioning of human sperm chromosomes 18 and 19 using fluorescent in situ hybridization (FISH). Preferred intranuclear positioning of chromosome territories (CTs) is proposed to be functionally important for differential genome activity in somatic cells during differentiation. In this Aim, sperm intra-nuclear positioning of chromosomes of similar base pair size, however strongly different in gene density, *Homo SApiens* (HSA) chromosomes 18 and 19 was determined. The working hypothesis was that, by analogy with somatic nuclei, gene rich HSA 19 will be positioned internally while gene poor HSA 18 will be positioned at the periphery of the sperm nuclei. The position of CHRs in the sperm nucleus may determine the time of their decondensation, remodeling and activation for transcription after fertilization.

5. Develop an approach for sperm CHR visualization of in zygotes. The sperm nucleus changes dramatically while the developing PN travels through the ooplasm and chromatin decondenses and recondenses. So far, methods of CHR visualization in the zygote, crucial for studies of male genome activation, have not been developed. Here, an application of the FISH approach to localize CHRs in developing mPN was developed and steps of sperm CHR unfolding in heterologous zygotes were described. In the future, these techniques will be applied to compare the kinetics of decondensation of sperm CHRs internally and peripherally positioned. The working hypothesis is that CHRs located on the periphery of the sperm nuclei will be withdrawn and decondensed prior to those located internally.

Summary of Findings

1. The best pair for heterologous ICSI to be used in these studies, hamster ova and Hsp, was ascertained.

2. The detailed kinetics of sperm chromatin decondensation within definite time intervals after ICSI in the hamster oocyte was established. Significant heterogeneity in mPN development was observed using injection of morphologically normal donor sperm.

3. It was demonstrated that sperm cells with removed acrosome, which models natural fertilization, decondense more rapidly and to a greater extent than acrosome intact cells.

4. The overall disappearance of PRMs from sperm is rather rapid and most likely completed within 1 hr in this heterologous ICSI system as demonstrated by immunofluorescent localization of PRMs 1 and 2. A marked zygote to zygote variability in mPN size for any time point post ICSI was observed. Also, PRM removal was shown to correlate with the developing PN area rather than time after injection.

5. Gene-poor HSA 18 was shown to be located in the periphery of the sperm nuclei and gene-rich HSA 19 was localized internally. Thus, the feature of CHRs radial positioning according to gene density observed in interphase is preserved in terminally differentiated sperm cells.

6. FISH protocol was established for the visualization of human CHRs in zygotes produced by the heterologous ICSI system in which Hsp was injected into hamster eggs. Mode of CHR unpacking resembles characteristic steps described earlier for artificially swollen sperm nuclei.

INTRODUCTION TO SPERM NUCLEAR BIOLOGY AND PATERNAL CHROMATIN REMODELING

Annually in the USA, more than 2 million conceptions are lost before the 20th week of gestation and approximately half of these carry chromosomal defects such as numerical abnormalities, partial duplications, deletions and inversions, etc. (McFadden & Friedman 1997, Wyrobek *et al.* 2005). About 10% of such chromosomal abnormalities are partly due to aberrations in ejaculated sperm (Hershlag 1992).

Infertile men often produce sperm with chromatin condensation defects as determined using cytochemical methods (Romano *et al.* 1998, Sakkas *et al.* 1998, Evenson & Wixon 2005). The reason for such deficiencies may be abnormal composition of basic chromosomal proteins (de Yebra *et al.* 1993, Bench *et al.* 1998). For example, mutations in PRMs (Iguchi *et al.* 2005) and PRM deficiency (Aoki *et al.* 2006) recently established in some infertile males may induce flawed chromatin organization. The roles of sperm chromatin organization and remodeling during successful fertilization start to emerge (Liu *et al.* 2002, Martianov *et al.* 2002).

Increased aneuploidy and chromosomal structural abnormalities have been reported in oligozoospermic patients (Schmid *et al.* 2004). Biochemical and FISH based diagnostic procedures for detection of chromosomal defects in germ-line cells and early embryos are either currently set up or being developed (Sloter *et al.* 2000, Fung *et al.* 2001, Shi & Martin 2001, Plachot 2003, Sloter *et al.* 2004, Tempest & Griffin 2004). Another previously unattended class of sperm CHR abnormalities may have an impact on fertilization and early embryo development. These aberrations are connected with: 1) atypical packing of CTs influencing the higher-order chromatin and CHR architecture; 2)

unstable or aberrant nuclear positioning of CHRs; and 3) disturbed telomeric or centromeric interactions (Mudrak *et al.* 2007; Zalensky & Zalenskaya 2007).

Modern reproductive technologies are enabling the treatment of infertile men with severe disturbances of spermatogenesis. The frequency of genetically and chromosomally defective sperm has become an issue of concern with increased usage of ICSI which is often used to treat these patients. Concerns are justified since sperm defects maybe directly carried to the embryo.

CHR organization in somatic cells

It is now well established that spatial distribution and structural organization of CHRs within eukaryotic nuclei at various stages of cell differentiation and cell cycle are dynamic, non-random, and tightly connected with gene regulation (Spector 2003, Foster & Bridger 2005).

Numerous studies of the last decades exploited DNA probes specific to individual CHRs or selected chromosomal domains to examine three-dimensional (3-D) genome organization using constantly improving FISH and microscopic techniques (Dernburg & Sedat 1998, Walter *et al.* 2006, Fraser & Bickmore 2007). It has been demonstrated that in the interphase nucleus, each CHR occupies a defined space referred to as a CT (Cremer *et al.* 1993, Cremer *et al.* 2004, Parada *et al.* 2004, Foster & Bridger 2005, Ramirez & Surralles 2008). Importantly, individual CTs are characterized by preferred intranuclear positions (Cremer *et al.* 2004, Misteli 2004, Verschure 2004, Fraser & Bickmore 2007, Fedorova & Zink 2009). A recent study reported that in diploid lymphoblasts and primary fibroblasts, gene-rich CHRs are preferably located at more internal regions, while the gene-poor CHRs concentrate towards the nuclear periphery

(Gilbert *et al.* 2005). The existence of the radial positioning suggests its functional relevance, most probably, to the control of gene expression.

The mechanisms by which genomes are spatially organized are unknown, several possibilities have been proposed: activity-driven self-organization, specific interactions with nuclear matrix/membrane and associations between heterochromatic domains (Parada *et al.* 2004). In addition, involvement of hypothetical protein complexes including nuclear actin, myosin, lamin and emerin was suggested (Mehta *et al.* 2008).

Organization of human sperm chromatin

The tight organization of the sperm chromatin is provided by interactions of the sperm DNA with PRM – highly basic proteins that almost completely replace histones during spermiogenesis. In humans, two types of highly basic chromosomal proteins, human PRM 1 (Hup 1) and human PRM 2 (Hup 2), are present in sperm nuclei. These PRMs are comprised of about 50-64 amino acids and are arginine and cysteine rich. Hup 1 and Hup 2 are responsible for the DNA supercompaction in sperm in which the DNA is six times more compact than in metaphase CHRs (Ward 2010).

Nucleoprotamine DNA is arranged into large toroidal subunits each containing approximately 50 kbp (Balhorn 2007). Histones remain associated with about 1-3% of the sperm DNA in all mammalian species studied except humans. In Hsp, histones constitute 10-15% of the total basic nuclear proteins (Tanphaichitr *et al.* 1978). It was shown, by digestion with nucleases, that in Hsp part of the DNA is organized by histones into nucleosomes (Banerjee *et al.* 1995, Zalenskaya *et al.* 2000, Nazarov *et al.* 2008). The particles obtained by a mild digestion with micrococcal nuclease contain telomere-specific DNA sequences (Zalenskaya *et al.* 2000). Recently it was demonstrated using

high-resolution genomic examination that this fraction is also enriched with gene sequences allegedly important for embryonic development (Arpanahi *et al.* 2009, Hammoud *et al.* 2009).

In summary, PRM are the key proteins that ensure tight packing of sperm CHRs, while residual histones bind the DNA sequences that could be important during and/or immediately after fertilization, participating in the initial stages of the mPN development.

CHR organization during spermatogenesis

Spermatogonia population is being constantly renewed by mitotic division. Experimental data on the chromosomal organization in the spermatogonia are scarce. For example, spermatogonia display compact CTs (Scherthan *et al.* 1996) and their telomeres (TEL) and centromeres (CEN) are dispersed throughout the nuclei as was shown in mouse, bovine and humans (Scherthan *et al.* 1996, Zalensky *et al.* 1997, Tanemura *et al.* 2005). It can be suggested that the general principles of CT organization in the spermatogonia would be similar to those of proliferating somatic cells.

A subgroup of spermatogonia that are committed to further differentiation undergoes a limited number of cell divisions and enters meiosis. Spermatogonia that cease continuous proliferation and move on to spermatocyte stage undergo two successive divisions, meiosis I and meiosis II. Genetic recombination at prophase I of meiosis I provide diverse combinations of parental genetic material. As a result of second division during meiosis II, four spermatids are formed: haploid germ line cells that transform to mature sperm during spermiogenesis.

In mammals, the complex process of differentiation of haploid spermatids into mature spermatozoa is supported by massive and radical reorganization of chromatin.

Most of the histones are replaced by PRMs (Meistrich *et al.* 1978, Meistrich *et al.* 2003, Govin *et al.* 2004), which results in extreme compaction of DNA within the sperm nucleus to a volume of about 5% of that in somatic cells.

Using FISH in the study of CHR arrangement during rat spermiogenesis Meyer-Ficca and colleagues (Meyer-Ficca *et al.* 1998) find that in the rat round spermatids of steps 1–9 both pericentromeric and telomeric signals are randomly dispersed throughout the nucleoplasm. At later stages, most TELs assemble around the nucleolus and pronounced TEL-TEL pairing markedly increases with further progression of spermiogenesis. During spermiogenesis, association of non homologous CENs was observed and a distinct chromocenter was shown to form in the nucleus of the mouse stages 3-4 spermatids.

CHR architecture and organization in mature human spermatozoa

The concept of the non-random CHR architecture in the nuclei of mature human spermatozoa has been developed based on earlier FISH and protein immunodetection studies (Zalensky *et al.* 1993, Haaf & Ward 1995, Zalensky *et al.* 1995, Zalensky *et al.* 1997). Hybridization with pan-centromeric probes and immunolocalization of CEN protein CENP-A demonstrated that CENs of all non-homologous CHRs are collected into the chromocenter that was localized to the nuclear interior (Zalensky *et al.* 1993). All TELs are positioned at the nuclear periphery where they interact with each other to form dimers and tetramers (Zalensky *et al.* 1997). Later it was found, using FISH with arm-specific subtelomere probes, that TEL pairs are formed through specific interactions between the two ends of the same CHR (Solov'eva *et al.* 2004).

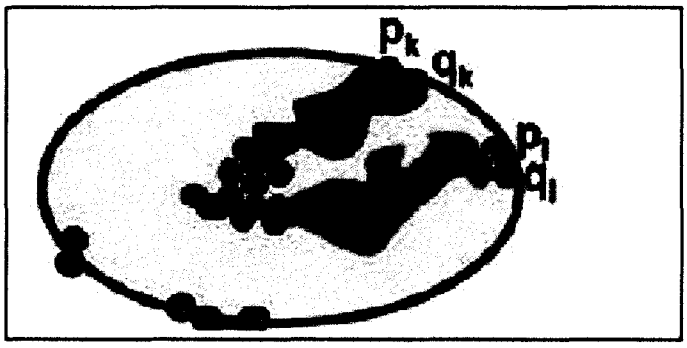

Figure 1 Model of chromosome organization in human sperm. Centromeres (red circles) are collected into chromocenter positioned in the nucleus interior; telomeres (green circles) interact in dimers at the nuclear periphery. Schematic paths of two CT are shown. Based on data of Zalensky et al., 1993; 1995; 1997; Haaf and Ward 1996.

The model of the Hsp nuclear architecture has been proposed according to which CTs are stretched between the chromocenter located centrally and TELs occupying nuclear periphery (Zalensky *et al.* 1995, Zalensky *et al.* 1997, Zalenskaya & Zalensky 2002; Fig. 1). According to this model, Hsp CHRs adopt a looped, hairpin conformation.

Internal organization of the sperm CTs was further studied in sperm cells subjected to controlled decondensation (Zalensky *et al.* 1993, Mudrak *et al.* 2005). This treatment causes partial unraveling of compact CT, thus allowing visualization of the inside structures. The extended territories of CHRs were found to be oriented parallel to the long nuclear axis and were formed by closely positioned *p*- and *q*-arms, either aligned or intertwisted. The chromosomal threads sharply bend in the vicinity of CENs, whereas the tips of *p*- and *q*- arms are located close to each other (Fig. 2). This observation is in line with the earlier discovery of specific interactions between p- and q- TELs (Solov'eva *et al.* 2004) and endorse the earlier proposed model of CT hairpin conformation in human spermatozoa.

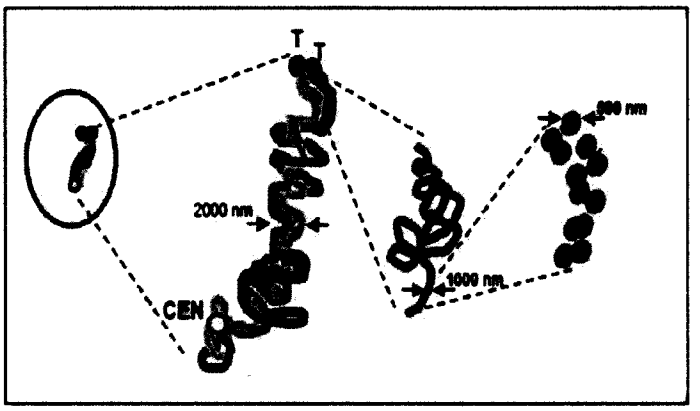

Figure 2 Levels of chromosome organization in human sperm based on FISH data. Model of hierarchical organization of chromosomes in human sperm nuclei. From left to right: compact CT, p- and q-arms are tightly merged; extended chromosome hairpin, antiparallel arms are interwined or stacked; 1000nm fiber of an individual arm; two rows of 500nm nodular structures that form 1000nm fiber. (Adapted from Mudrak et al. 2005).

Although, in contrast to somatic cells, spermatozoa are genetically inactive, about 10 years ago evidence of non-random spatial positioning of CTs in Hsp started to emerge (Gurevitch *et al.* 2001, Hazzouri *et al.* 2000, Sbracia *et al.* 2002, Tilgen *et al.* 2001). CT localization was performed using either CHR-specific near-CEN (Hazzouri *et al.* 2000, Zalenskaya & Zalensky 2004) or more recently whole CHR painting probes (Zalenskaya & Zalensky 2004, Mudrak *et al.* 2005, Manvelyan *et al.* 2008). CHRs in Hsp display radial positioning - for example, locations of HSA 7 and HSA 6 CENs are mostly peripheral while those of HSA 16 and HSA X are more internal (Zalenskaya & Zalensky 2004). Analogous to somatic cells, radial intranuclear positioning seems to be driven by gene density (Manvelyan *et al.* 2008). Since sperm nuclei in many mammals have a polarized extended shape with two poles: apical (acrosomal) and basal (tail attachment) it is possible to access the longitude positioning of CTs. This has been done for human

(Zalenskaya & Zalensky 2004, Mudrak *et al.* 2005, Manvelyan *et al.* 2008) and boar (Foster *et al.* 2005) spermatozoa. Existence of longitude positioning may be a factor important in process of artificial fertilization using ICSI technique.

Fertilization

Fertilization converts two terminally differentiated cells into a totipotent zygote that can form all the cell types in the body. Human eggs, like those of most mammals, are fertilized at meiotic metaphase II. Fertilization activates the oocyte and triggers the completion of meiosis so that the inactive sperm nucleus is, in a coordinated fashion, transformed into a functional mPN within the egg cytoplasm. This process consists of complex overlapping stages (Collas & Poccia 1998, Sutovsky & Schatten 2000, McLay & Clarke 2003): (1) removal of the sperm nuclear envelope and disassembly of nuclear lamina; (2) substitution of PRMs with histones that leads to initial chromatin decondensation followed by recondensation; (3) rebuilding of a nuclear envelope; (4) swelling of the mPN and its migration towards the female PN; and (5) the rapid demethylation of sperm DNA during PN development (Fulka *et al.* 2004). And finally paternal and maternal genomes unite and prepare for cleavage forming the mitotic spindle. At fertilization, the oocyte faces the challenge of remodeling the condensed sperm chromatin into an accessible, transcriptionally competent form. Upon entry into the oocyte, the sperm nucleus undergoes marked morphological changes. This remodeling follows a characteristic tri-phasic pattern (Wright & Longo 1988; Adenot *et al.* 1991). In the first phase, during the period that the oocyte is completing anaphase II, the paternal chromatin disperses. Although the change in volume is difficult to calculate, the area occupied by the chromatin increases threefold. While the oocyte CHRs are

completing telophase II, the sperm chromatin transiently recondenses into a small mass, the area it occupies decreasing by one-half. In the final phase, the chromatin extensively decondenses within the male pronucleus and the area it occupies increases 10-fold. Morphological remodeling is accompanied by incorporation, modification and even decomposition of sperm chromosomal proteins. Steps of sperm chromatin remodeling are outlined in Fig. 3. The replacement of PRMs by histones is driven by oocyte-derived

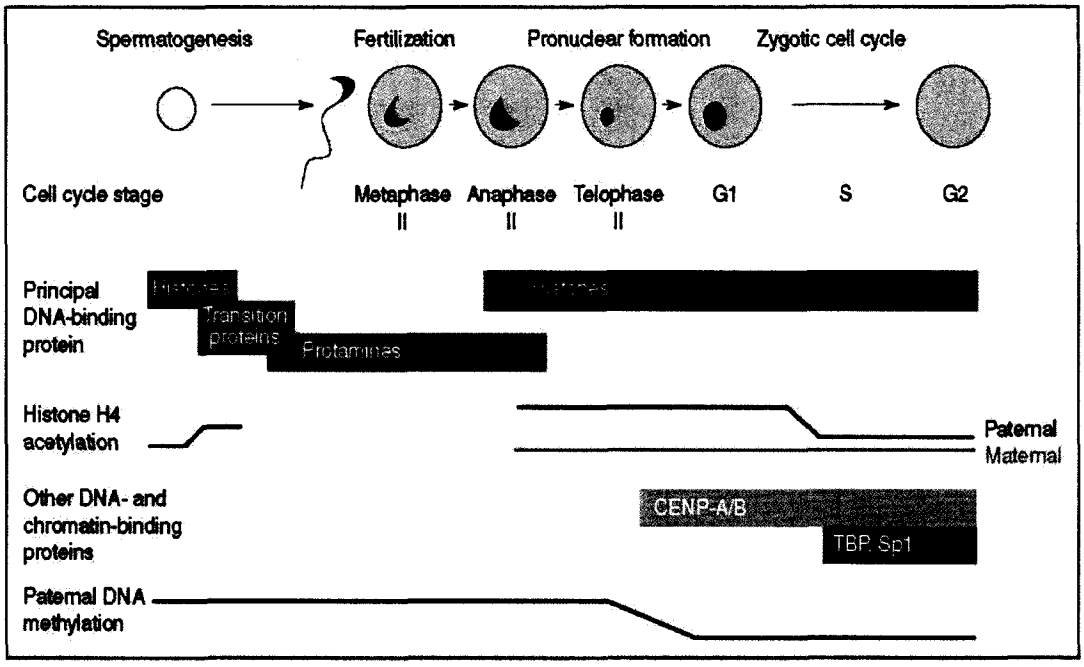

Figure 3 Summary of sperm chromatin remodeling in mammals. During spermatogenesis, sperm histones are replaced by transition proteins, which are then replaced by protamines. After fertilization, the protamines are replaced by oocyte-supplied histones. This replacement occurs as the oocyte completes the second meiotic division and coincides with a transient recondensation of the paternal chromatin. The paternal and maternal chromatin then decondense extensively within separate pronuclei, and the histones on the paternal chromatin become deacetylated. Other oocyte proteins (centromeric proteins CENP-A/B, and transcription factors TBP and Sp1) imported into the pronuclei further modify the chromatin and DNA replication begins. (Adapted from McLay & Clarke 2003).

factors that facilitate decondensation of paternal chromatin. This process is poorly studied and involves disruption of PRM sulphydryl bonds and probably protein chaperons of the nucleoplasmin type (Nakazawa *et al.* 2002). Old data indicated that PRMs are removed from sperm chromatin and substituted with histones by the end of oocyte anaphase II (Ecklund & Levine 1975, Kopencny & Pavlok 1975, Rodman *et al.* 1981). The precise timing of histone to PRM exchange on to the paternal chromatin at fertilization has yet to be established using modern techniques. From general principle it may be suggested that after histone assembly and chromatin organization into nucleosomes, the paternal genome becomes decondensed within the mPN.

PRELIMINARY RESULTS

Earlier studies from our laboratory used FISH to visualize CHRs in sperm artificially swollen with heparin and in the presence of dithiothreitol (DTT) (Zalensky *et al.* 1993). DTT cleaves disulfide bonds between PRM and thus loosens chromatin structure. The exact mechanism of heparin action is unknown but it is proposed (Jager *et al.* 1990; Villepoteau 1992) that it weakens DNA-basic protein, here DNA-PRMs. Such an approach allows imaging of sperm CHR organization as illustrated by an example in Fig. 4.

It was not clear to what extent such artificial procedure of sperm swelling reflects processes of mPN development during fertilization. Therefore, another approach was explored: decondensation of Hsp in cell free extracts from *Xenopus Laevis* eggs (XEE). This cell-free system was originally developed to study the mechanisms involved in transformation of amphibian sperm nuclei after fertilization (Lohka and Masui 1983, Iwao and Katagiri 1984, Ohsumi *et al.* 1988). It was shown that incubation of DTT-

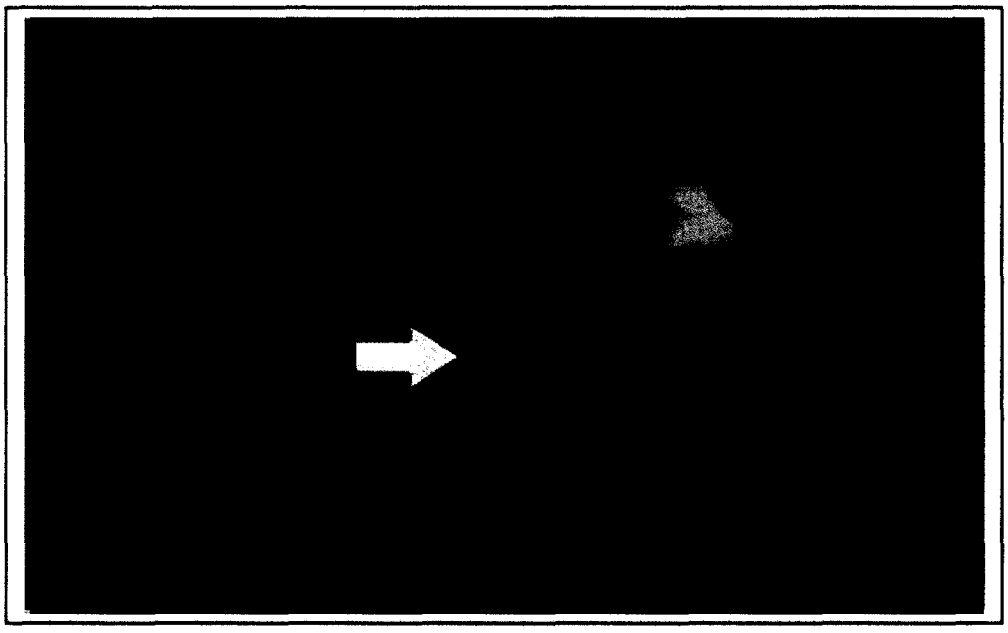

Figure 4 FISH visualization of sperm chromosomes. Unpacking of HSA 1. Human sperm cells at two stages of decondensation induced by heparin/DTT treatment- minimal (left image) and highly decondensed (right) FISH using HSA 1 arm-specific painting probes (p-arm green, q-arm red). Total DNA counterstained with DAPI (blue).

pretreated and permeabilized Hsp in XEE resulted in chromatin decondensation, DNA synthesis and subsequent chromatin condensation (Brown *et al.* 1987, Montag *et al.* 1992, Neuber *et al.* 1999). In these experiments, lysolecithin permeabilized and DTT treated Hsp cells were incubated in XEE for various periods of time, aliquots were withdrawn, loaded onto slides, and fixed. Sperm nuclei progressively decondense in parallel with the withdrawal of PRM by XEE components (Fig. 5A). Maximum enlargement was achieved at ~30 min of the incubation and then the nuclei shrunk. FISH shows how the initially compact territory of HSA 6 was gradually dispersed during the incubation (Fig. 5B).

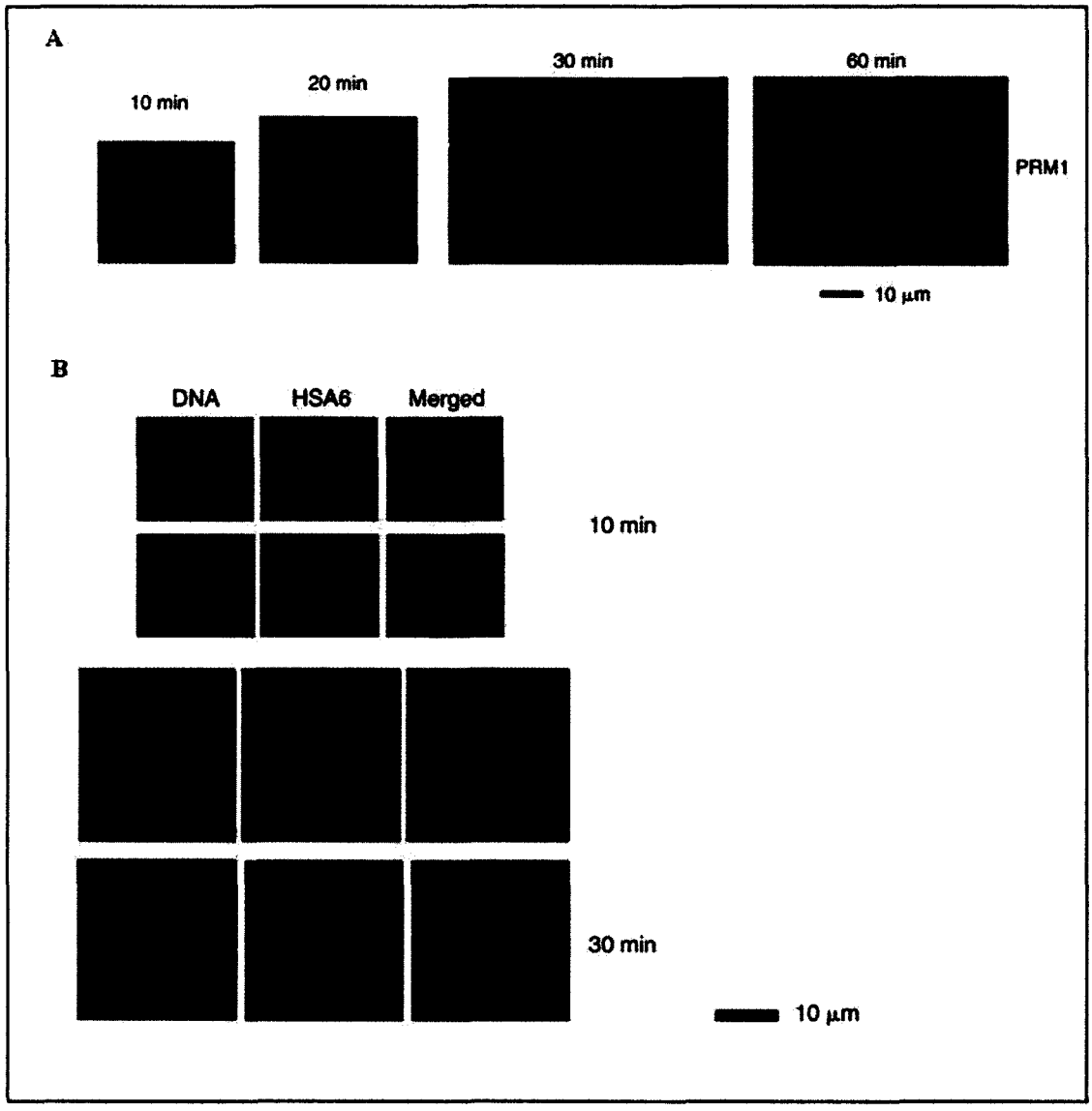

Figure 5 Transformations of human sperm nuclei in Xenopus egg extracts. (A) Immunolocalisation of PRM 1. Images were captured using selective or triple-band pass filters. Upper rows: total DNA counterstained with DAPI (blue); lower rows: PRM 1 immunostaining (red); middle rows: merge images acquired using a triple-band pass filter. Incubation times are indicated on the top. (B) Unpacking of the sperm HSA6 territory. FISH using painting probe (green), total nuclear DNA counterstained with DAPI (blue). (Adapted from Mudrak *et al.* 2009).

Although the *in vitro* approaches can give some information about Hsp CHR behavior during early events of fertilization, they are far from the real picture for several

reasons. In XEE for example, some ooplasm factors may be absent or unable to be properly organized in space, not to mention species-specific differences between *Xenopus* and humans. Therefore the goal of this work was to find the optimum oocyte system that will yield the closest model of the events that occur during human fertilization. Limited literature data indicated that the use of a heterologous ICSI model may be the more physiological approach compared to cell-free extracts. Understanding the dynamics and mechanisms of Hsp genome spatial organization during fertilization may be advantageous for improvements in assisted reproductive technologies for the infertile male. Important for future experiments, the preliminary data resulted in the adjustment of established FISH techniques to observe decondensing sperm CHRs in ooplasm-like milieu.

CHAPTER II

DEVELOPMENT OF A HETEROLOGOUS ICSI MODEL TO STUDY SPERM CHROMOSOME TRANSFORMATION DURING FERTILIZATION

INTRODUCTION

The first ICSI in mammals was reported over thirty years ago (Ueharea & Yanagimachi 1976); hamster spermatozoa were injected into mature hamster oocytes (HO) and transformation of the sperm head into an mPN was observed. Since then, in mammalian species such as rabbit (Hosoi *et al.* 1988, Iritani & Hosoi 1989), cattle (Gotto *et al.* 1990, Hamano *et al.* 1999), mouse (Kimura & Yanagimachi 1995), monkey (Hewitson *et al.* 1999), human (Palermo *et al.* 1992, Van Steirteghem *et al.* 1993), hamster (Yamauchi *et al.* 2002), live offspring have been obtained from oocytes fertilized by ICSI.

The application of ICSI re-invigorated the study of inter-species fertilization. Such heterologous ICSI is theoretically a good model to study the mechanism of sperm-oocyte nuclear fusion, oocyte activation and early events of fertilization for species where homologous ICSI is not possible, namely the human. Sperm nuclei from humans, mice, chinchillas, bulls and rats were microinjected into HO and sperm nuclear decondensation and mPN formation was observed by phase contrast microscopy (Perreault *et al.* 1988). The mPN also formed after injecting mouse, bovine or Hsp cells into porcine oocytes (Kim *et al.* 1999). Mouse and HO have been used to study decondensation, chromatin changes and the transformation of human spermatozoa (Goud *et al.* 1998, Hewitson *et al.* 1997, Lee *et al.* 1996). Heterologous ICSI of bovine oocytes (BO) with Hsp was

reported to be applicable to study the human mPN development and centrosomal function at fertilization (Nakamura *et al.* 2001, Terada 2004). Thus, heterologous ICSI may be a useful technique for basic research concerning human male gametes at fertilization.

Since bovine fertilization resembles human fertilization by having paternally derived centrosomes (Sathananthan *et al.* 1997), heterologous ICSI using BO is a promising model to study the Hsp nuclear transformation. A known problem with bovine ICSI is the need for additional oocyte activation in order to achieve developmental competence. Accordingly, homologous or heterologous bovine ICSI has been combined with different schemes of oocyte activation: electrical stimulation (Hwang *et al.* 2000), chemical activation with ethanol (Hamano *et al.* 1999) or ionomycin (Rho *et al.* 1998) or by combination of these stimuli with cyclohexamide (Suttner *et al.* 2000) or 6-dimethylaminopurine (Rho *et al.* 1998, Chung *et al.* 2000).

Additionally, various chemicals such as heparin (Keefer *et al.* 1990, Chen & Seidel 1997, Wei & Fukui 1999), caffeine (Gotto 1990, Wei *et al.* 1999, Iwasaki & Li 1994), strontium (Meo *et al.* 2007), lysolecithin (Neuber *et al.* 1999, Mudrak *et al.* 2009), and calcium ionophore (Chen *et al.* 1997, Wei *et al.* 1999) were applied to sperm to be used for ICSI. These chemicals are able to increase sperm membrane permeabilization, induce acrosome reaction, and promote sperm head decondensation. Widely used in sperm pretreatment is DTT which reduces PRM disulfide bonds and leads to decondensation of the sperm head (Calvin & Bedford 1971, Bedford & Calvin 1974, Sutovsky & Schatten 1997, Tateno & Kamiguchi 1999) and thus may promote mPN development in sperm-injected oocytes.

The main goal of this work is to develop a heterologous ICSI approach to investigate the transformation of the human paternal genome at fertilization. In this section, the study was designed to determine which heterologous ICSI model utilizing HO and BO would yield the most efficient, high rate of human mPN formation. To optimize zygote development, pretreated Hsp and various forms of chemical and physical oocyte activation were utilized paying major attention to mPN formation.

MATERIALS AND METHODS

Preparation of eggs

Hamster. Frozen HO (Conception Technologies, San Diego, CA, USA) were thawed and washed for 10 min in mHTF supplemented with 10% SSS (mHTF-SSS, modified Human Tubal Fluid plus Synthetic Serum Substitute, Irvine Scientific, Santa Ana, CA, USA) at room temperature (RT) before being placed into P1 medium (Irvine Scientific) supplemented with 10% SSS. Viable oocytes were incubated at 37°C in 5% CO_2 prior the ICSI procedure.

Bovine. Fresh BO (BOMED, Inc., Madison, WI, USA) were incubated 20-24 hr in maturation buffer provided by the vendor. Cumulus-corona complexes were removed with 0.1% hyaluronidase solution and gentle pipetting. Oocytes with a first polar body were placed in TCM199 (Sigma, St. Louis, MO, USA) supplemented with 10% fetal bovine serum (Sigma) and incubated at 39°C in 5% CO_2 prior to any further manipulations.

Preparation of spermatozoa

Semen samples were obtained from three normozoospermic (WHO 1992) healthy men enrolled in the donor sperm program at The Jones Institute for Reproductive

Medicine. The study was approved by the Institutional Review Board of Eastern Virginia Medical School and written informed consent was obtained from all participants. Spermatozoa in all samples had normal morphology (>30% normal forms based on WHO criteria; WHO 1992).

After liquefaction, the semen sample was washed with HTF (Human Tubal Fluid, Irvine Scientific, Santa Ana, CA, USA) supplemented with 3% BSA (Bovine Serum Albumin, Sigma, St. Louis, MO, USA). The spermatozoa were washed twice with HTF–BSA and centrifuged for 10 min at 300g. After the second wash, the supernatant was removed and the pellet was overlayed in fresh HTF–BSA. A swim-up procedure was performed at 37°C, 5% CO_2 for 1 hr. Next, washed sperm cells were treated with 1mM MitoTracker green FM or red (Molecular Probes, Eugene, OR, USA) for 15 min at 37°C for visualization of the sperm tail in subsequent microscopy. For hamster heterologous ICSI, non-treated swim-up sample was used for injections as hamster ICSI does not require further sperm/oocyte activation for mPN development.

In bovine heterologous ICSI experiments, after swim-up, capacitation was conducted in HTF-BSA at 37°C, 5% CO_2 for 5 hr. The motile sperm fraction was then divided into various treatment groups: 1) frozen/thawed (-80°C); 2) DTT (0.5 mM); 3) calcium ionophore (10 uM); 4) lysolecithin (40 ug/ml) and 5) DTT + calcium ionophore. Such pretreatment of sperm has been reported to promote zygote development (Rho *et al.* 1998, Suttner *et al.* 2000, Wei *et al.* 1999).

Oocyte Activation and ICSI

For injections using HO, conventional ICSI was performed as previously described (Palermo *et al.* 1992). Briefly, 1µl of sperm suspension was diluted with 4 µl of

10% polyvinyl pyrolidone (PVP-Irvine Scientific) and placed in the center of an injection dish. Each frozen-thawed mature (metaphase II) HO was placed in 5 µl of mHTF-SSS surrounding the central drop containing the sperm suspension and covered with mineral oil. HO were injected using Narishige micromanipulators (Narishige, Tokyo, Japan) mounted on a phase-contrast inverted microscope (Olympus, Tokyo, Japan) at 400x magnification (Fig. 6). The selected spermatozoon was aspirated into the injecting micropipette and introduced through the zona pellucida into the ooplasm. A small amount of ooplasm was aspirated into the pipet to ensure breaking of the oolemma. The micropipette was then slowly withdrawn and the injected oocytes were kept at 37°C in 5% CO_2 for 16 hr in P1 medium (Irvine Scientific) with 10% SSS. Viable oocytes were fixed with 2% paraformaldehyde (Sigma) and stained for evidence of an mPN.

For heterologous ICSI using BO, both conventional and Piezo ICSI were utilized as injection methods. The technique, Piezo ICSI, incorporates electrical pulses to propel the injection needle into the oocyte making ICSI more efficient in comparison to conventional manual needle introduction especially for species like bovine (Katayose *et al.* 1999). Piezo ICSI is similar to conventional ICSI except the needle holder for injection is attached to the drive unit of a piezo-micromanipulator (PMM: Prime Tech Ltd, Tsuchiura, Ibaraki, Japan; Fig 6). The drive unit of the piezo-micromanipulator was driven by a controller (PMAS-CT-150: Prime Tech Ltd). Briefly, a captured motile spermatozoon was immobilized by giving piezo pulses to sperm tail in 10% PVP drops. An immobilized spermatozoon was aspirated into the injection needle by its tail and transferred into the mHTF (Irvine Scientific), after which ICSI was conducted. At first, the needle was allowed to penetrate only the zona pellucida while piezo pulses (five to 10

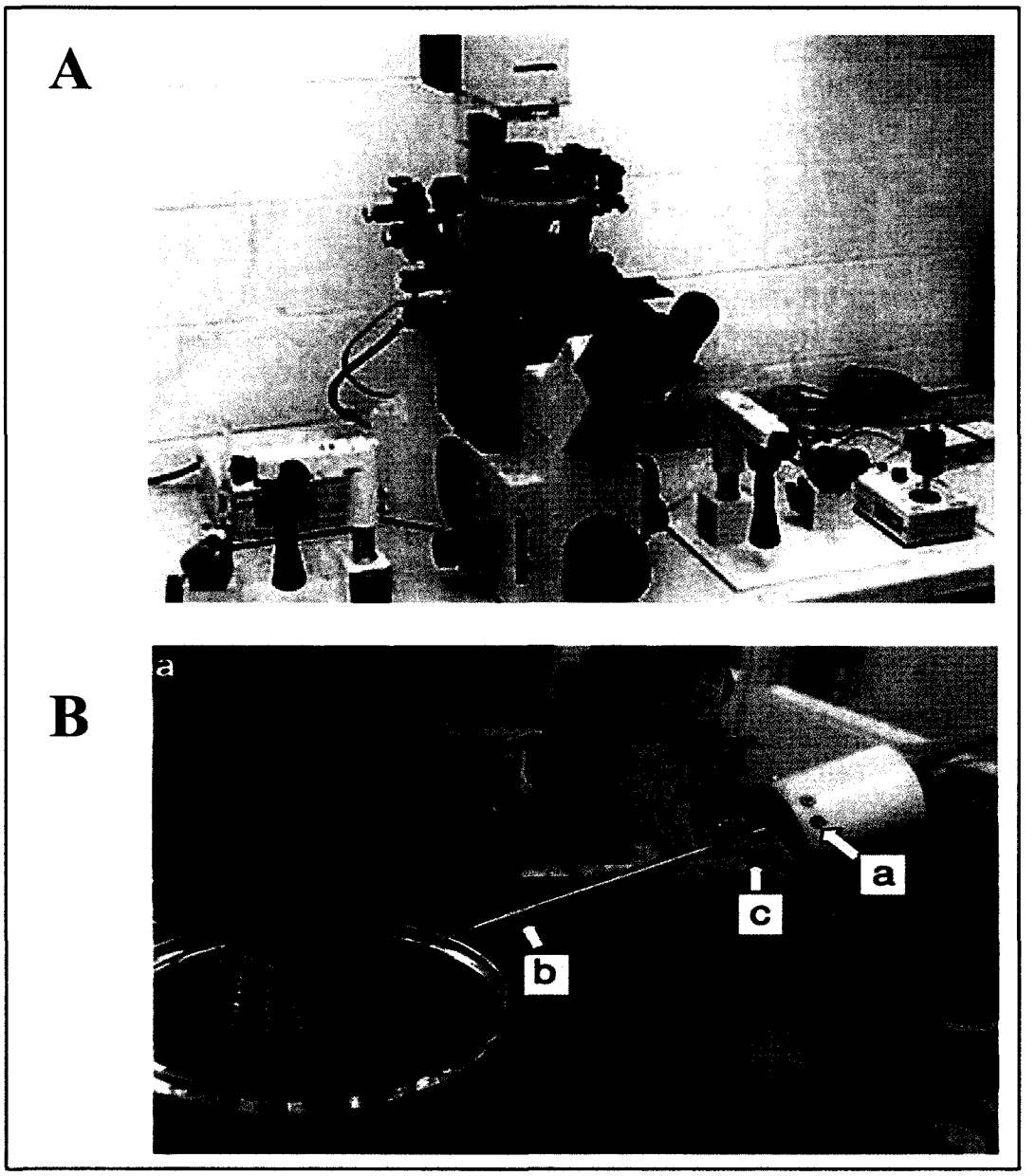

Figure 6 Micromanipulator set-up for heterologous ICSI. (A) Conventional ICSI set-up for HO injections. (B) Piezo ICSI apparatus showing (a) piezoelectric drive unit, (b) micro pipet holder and (c) tension screw. Piezo ICSI was used for BO injections to produce more efficient zygote development.

pulses, about 0.5 Hz) were applied. Then the needle was allowed to penetrate deeply into the ooplasm without applying piezo pulses, and when the oolemma extended sufficiently it was punctured with one piezo pulse. The puncture of the oolemma was confirmed by the ability of the oolemma, which had been brought into the oocyte as the needle was inserted into the oocyte, to return to its original position. No suction of ooplasm was performed during the injection of a spermatozoon. Oocytes were incubated 16 hr post ICSI at 39°C 5% CO_2 in TCM199 (Sigma) supplemented with 10% fetal bovine serum (Sigma) then fixed and stained for visualization of sperm nucleus.

According to some authors (Rho *et al.* 1998, Chung *et al.* 2000, Horiuchi *et al.* 2002) bovine ICSI requires activation of the oocytes as a prerequisite for PN formation. As such, a combination of pretreated sperm was used as previously described with various oocyte pretreatments: 1) ethanol (ETOH) (4 hr post ICSI); 2) calcium ionophore (A23187) (50 uM); 3) DTT (0.5 mM); 4) strontium (10 mM). In the ETOH activated oocyte group, oocytes were incubated in standard culture conditions for 4 hr post ICSI then incubated for 5 min in medium supplemented with 7% ETOH at 39°C, washed twice, then returned to culture until fixation at 16 hr post insemination. For calcium ionophore activation, oocytes were transferred after injection to culture medium containing 50 uM A23187 for 5 min at 39°C, washed twice. This procedure was repeated two more times each after 30 min intervals then returned to culture until fixation at 16 hr post ICSI. In the DTT treated group, injected oocytes were incubated for 16 hr at 39°C in standard culture medium supplemented with 0.5 mM DTT then fixed. The strontium activated oocytes were incubated for 4 hr at 39°C in standard culture medium containing 10mM strontium, washed twice then returned to culture and fixed at 16 hr post injection.

Experimental Design

The study was comprised of two sets of experiments. In the first experiment, mPN development in HO injected with Hsp was examined. In experiment two, BO were used as acceptor cells and the effects of sperm treatments and oocyte activation schemes on subsequent sperm head decondensation in the heterologous zygote were compared. Conventional and piezo ICSI were used.

Observation of pronuclei development

Zygotes were withdrawn from culture at designated times and fixed with 2% paraformaldehyde (Sigma). Zygotes were washed in PBS and mounted in a small volume of Vectashield (Vector Laboratories, Burlingame, CA, USA) supplemented with 4-,6-diamidino-2-phenylindole (DAPI) to visualize total DNA.

Microscopy and data analysis

Zygotes were observed using a UV microscope (Leitz Ortholux,Wetzlar, Germany) with selective DAPI filter and oil immersion 60×1.4 numerical aperture objective. Images were collected using a MagnaFire digital color camera and MicroFire software (Optronics, Goleta, CA, USA). Images were processed in Adobe Photoshop 7.0 (Adobe Systems, San Jose, CA, USA). The surface area of mPN stained with DAPI was measured using Image J soft ware (National Institute of Mental Health, Bethesda, Maryland, USA). Areas of sperm/mPN were evaluated on the analyzer screen. After interactive demarcation of the circumference of the nuclei, the surface areas were automatically calculated by utilizing the enclosed pixels areas.

RESULTS

In experiment 1, in which 76 HO (3 replicates) were injected with non-treated Hsp, the majority of oocytes (70.1%) survived. These oocytes were cultured as described in Methods section and examined by DNA staining at 16 hr post ICSI. 69.8% of the oocytes demonstrated mPN development (Fig 7).

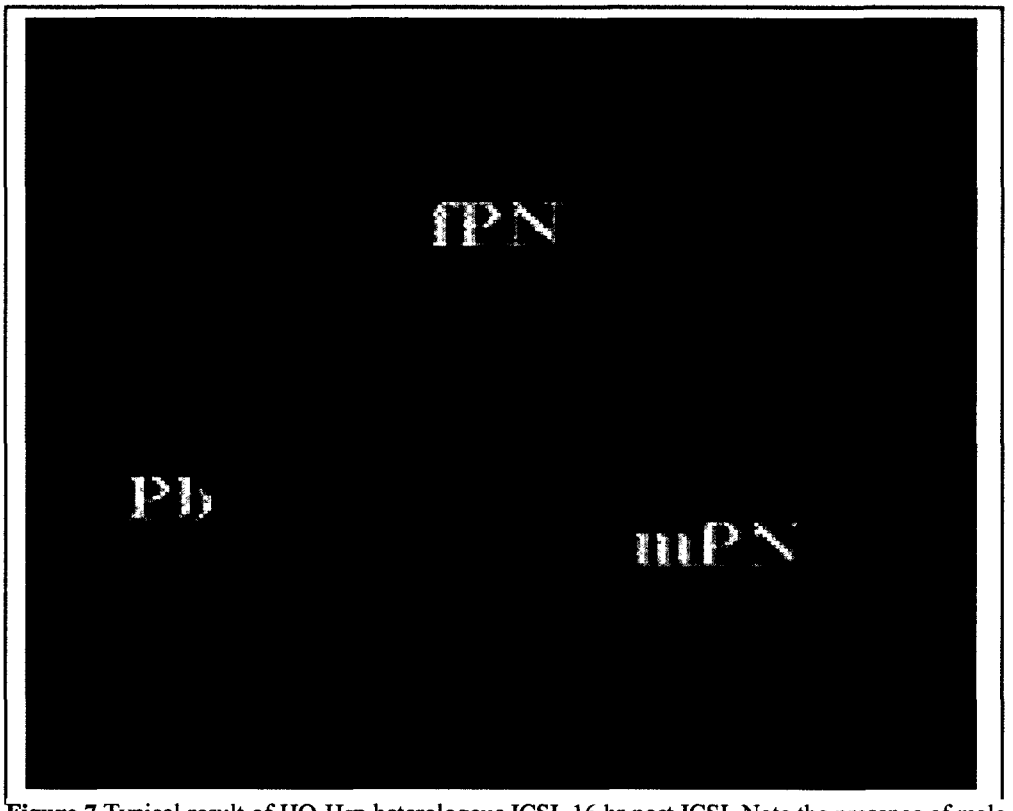

Figure 7 Typical result of HO-Hsp heterologous ICSI, 16 hr post ICSI. Note the presence of male pronucleus (mPN) and female pronucleus (fPN). Total DNA stained with DAPI, blue. Scale bar = 10 μm.

In the second experiment, the rate of mPN development in the Hsp-BO ICSI was determined. In the initial set, 34 BO (2 replicates) were injected using conventional ICSI

with Hsp and activated after 4 hr incubation by placing the injected oocytes in culture medium supplemented with 7% ETOH for 5 min. Oocytes were then washed and re-cultured overnight prior to fixation with 2% paraformaldehyde (Sigma). After 12 hr of further incubation, egg activation was detected using DAPI staining by the presence of fPN and mPN. Hsp did not decondense in any of the injected oocytes (Fig. 8).

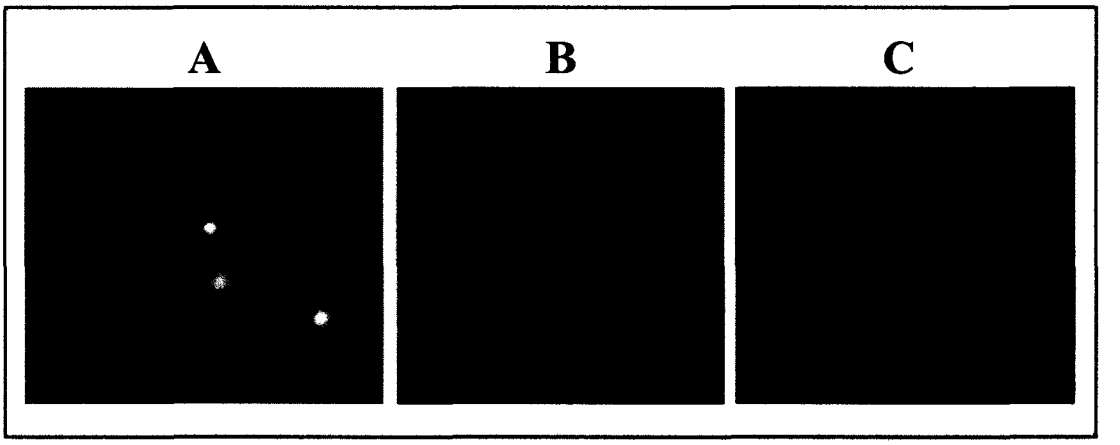

Figure 8 Typical result of BO-Hsp heterologous ICSI. Non-treated Hsp, zygote activated with ETOH at 4 hr post ICSI and fixed at 16 hr. (A) Phase contrast image showing presence of female pronucleus (fPN), first polar body (PB) and condensed sperm (Sp). (B) Total DNA stained with DAPI, blue. (C) Sperm tail is stained with mitotracker (red). Scale bar = 20 μm.

Next, different methods of sperm pretreatment and oocytes treatment post ICSI using different activating agents was explored. 186 oocytes were divided into six treatment groups (31/group; 2 replicates): 1) DTT-treated sperm + ETOH activation; 2) DTT+ ionophore-treated sperm + ionophore activation; 3) ionophore-treated sperm + ionophore activation; 4) lysolecithin-treated sperm + ionophore activation; 5) lysolecithin-treated sperm + strontium activation; 6) frozen/thawed sperm + ionophore

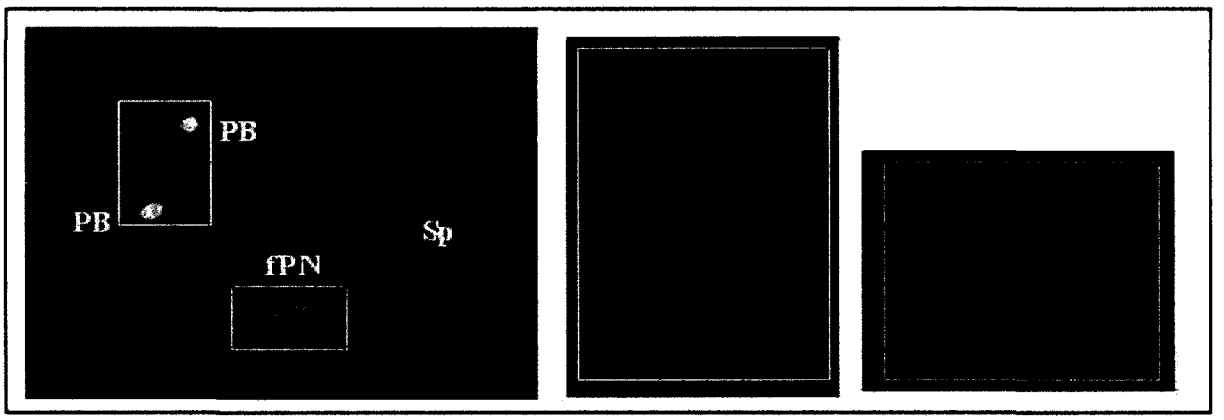

Figure 9 BO-Hsp heterologous ICSI. DTT-treated Hsp, zygote activated with ETOH at 4hr post ICSI and fixed at 16hr. Note oocyte activation demonstrated by formation of two polar bodies (PB) and the presence of a female pronucleus (fPN). Sperm head (Sp) remains condensed. Total DNA stained with DAPI, blue. Right panels show enlargement of two PB (white box) and fPN (yellow box). Scale bars = 20 μm.

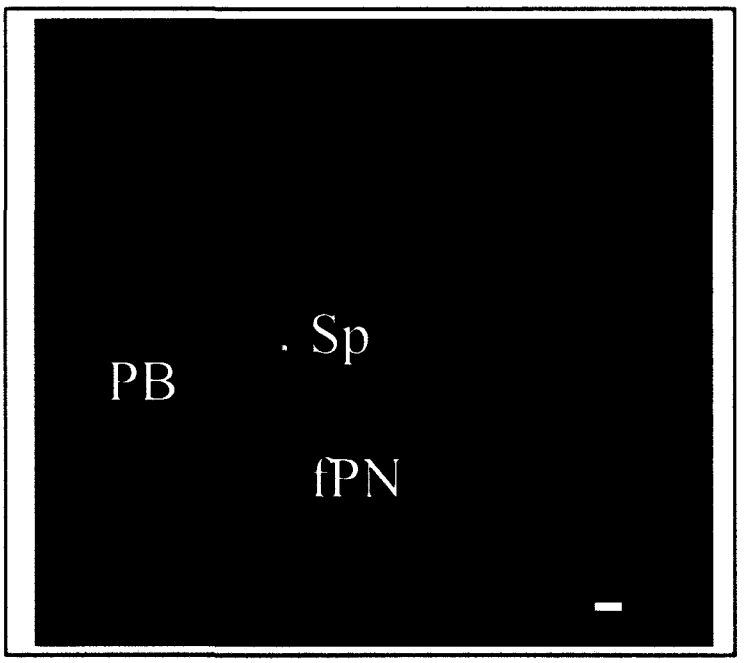

Figure 10 BO-Hsp heterologous ICSI. Hsp pretreated with DTT + ionophore, zygote activated with ionophore 3x10 min post ICSI. Note the presence of female pronucleus (fPN) indicating egg activation. No sperm (Hsp) decondensation was observed. Total DNA stained with DAPI, blue. Scale bar = 20 μm.

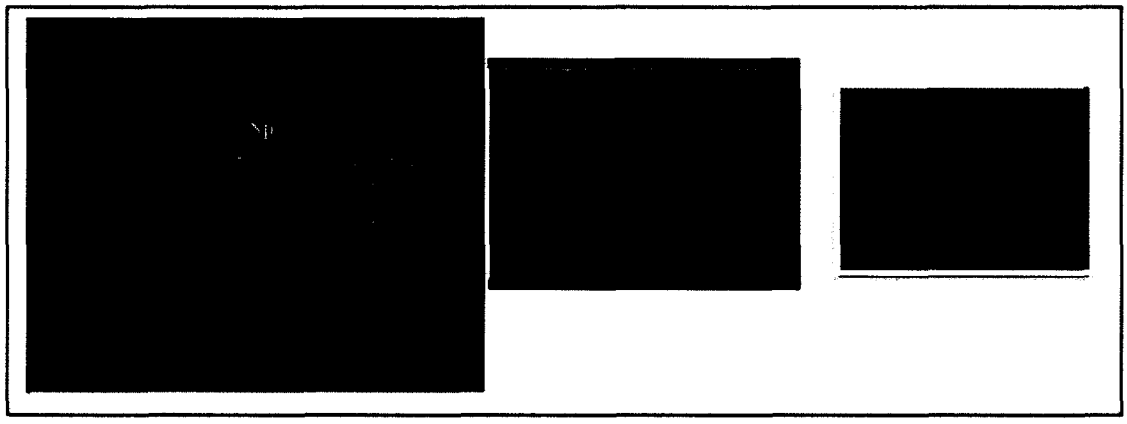

Figure 11 BO-Hsp ICSI. Hsp pretreated with 0.5 mM DTT + lysolecithin zygote activated with ionophore 3x10 min post ICSI. Note the presence of condensed sperm (Sp) and two pronuclei (PN) in white box indicating parthenogenetic activation. Yellow box illustrates presence of two polar bodies (PB). Right panels enlarged from white and yellow boxes, respectively. Total DNA staining with DAPI (blue). Scale bar = 20 μm.

activation. The use of pretreated sperm and either ETOH, ionophore or strontium oocyte activation did yield oocyte activation; however no sperm decondensation was observed (Figs. 9, 10, 11; Table 1). As no sperm head decondensation was observed in these experiments, 178 BO were injected using Piezo ICSI with the same set of pretreated sperm/oocyte activation groups. Again, no mPN development was observed (Table 1).

DISCUSSION

The data shown here on HO-Hsp heterologous ICSI demonstrated successful development of mPN in ~70% of zygotes, which is in line with previously reported data (Ahmadi & Ng 1997, 1999). Therefore, this system may be used for the planned studies of human male CHR transformation following fertilization.

Rodents including hamster have maternal inheritance of centrosome unlike humans and other mammals (Schatten *et al.* 1991). It is unlikely that the centrosome

Table 1 Zygote development in different treatment groups after human sperm ICSI into bovine oocytes

Type of ICSI	Activation group Sperm + oocyte	No. of oocytes examined (n)	Decondensed sperm (presence of mPN) [n (%)]	Oocytes with fPN [n (%)]	Oocytes with 2 PB [n (%)]
Conventional N= 34	None + ETOH	34	0 (0)	3 (8.8)	2 (5.9)
Conventional N= 186	DTT + ETOH	31	0 (0)	4 (12.9)	3 (9.6)
	(DTT + Ion) + Ion	31	0 (0)	3 (9.6)	2 (6.5)
	Ion + Ion	31	0 (0)	2 (6.5)	1 (3.2)
	Lys + Ion	31	0 (0)	2 (6.5)	2 (6.5)
	Lys +Str	31	0 (0)	3 (9.6)	3 (9.6)
	Frozen/Thawed + Ion	31	0 (0)	2 (6.5)	0(0)
Piezo N= 178	DTT + ETOH	29	0 (0)	8 (27.6)	2 (6.9)
	(DTT + Ion) + Ion	29	0 (0)	6 (20.7)	3 (10.3)
	Ion + Ion	30	0 (0)	5 (16.7)	3 (10)
	Lys + Ion	30	0 (0)	4 (13.3)	2 (6.7)
	Lys +Str	30	0 (0)	7 (23.3)	4 (13.3)
	Frozen/Thawed + Ion	30	0 (0)	4 (13.3)	0 (0)

Treatment groups: ETOH – ethanol; DTT- dithiothreitol; Ion – calcium ionophore (A23187); Lys- lysolecithin; Str- strontium. Nuclear changes: mPN = male pronucleus; fPN = female pronucleus; PB = polar body.

All zygotes fixed 16hrs post ICSI.

participates in mPN CHR transformation. Nevertheless, keeping this in mind, we also explored the heterologous Hsp-BO system.

Injection of 398 BO with Hsp and using different combinations of sperm/oocyte pretreatment, which may promote activation of zygote development, did not produce formation of mPN in ooplasm (Table 1). Application of Piezo injection did not change overall results as well. These data are in contrast with the results reported in several

publications from Dr. Terada's laboratory (Nakamura *et al.* 2001, Terada 2004, Yoshimoto-Kakoi *et al.* 2008, Terada *et al.* 2009). Interestingly, other groups have reported that in bovine the rate of blastocyst development following homologous ICSI is not higher than 12-20% (Horiuchi *et al.* 2002, Keskintere & Brackett 2000). The reason may be the state and quality of the BO. Nakamura et al. (2001) used oocytes collected from local slaughterhouse and in vitro matured in their laboratory while oocytes supplied by a company (BOMED) were used in this work. These oocytes were collected in Wisconsin and shipped overnight in an undisclosed maturation medium using a temperature controlled chamber. Differences in the maturation procedure could be a contributing factor to the lack of mPN development we experienced.

Other possible reasons for such a low developmental capacity of embryos after ICSI cannot be excluded: 1) an incomplete activation of the oocyte; 2) inappropriate capacitation of sperm before injection that does not allow the release of sperm factors responsible for oocyte activation (Stricker 1999) and/or results in the block of sperm head decondensation.

In summary, these findings indicate that in hamster/human heterologous ICSI, the vast majority of the zygotes demonstrated sperm nuclear decondensation/mPN development (Fig. 7). However, such development in the Hsp-BO model was not attained. Thus, it was established that HO-Hsp ICSI is robust and suitable for the planned studies, yielding the most efficient formation of mPN.

CHAPTER III

KINETICS OF HUMAN MALE PRONUCLEAR DEVELOPMENT IN A HETEROLOGOUS ICSI MODEL

INTRODUCTION

The ability of Hsp to form PN within zona-free HO, the "hamster test" or HO sperm penetration assay (Yanagimachi *et al.* 1976, Rogers *et al.* 1983, Aiken 1984, Hewitson *et al.* 1997) has been used by IVF clinics for years. In more recent modifications, a single Hsp is injected into each oocyte using the ICSI technique, which eliminates any sperm bound to oocyte surface (Yanagida *et al.* 1991). After injection, Hsp undergoes decondensation that, at first glance, mimics the formation of PN. Another system of heterologous ICSI of Hsp into mouse oocytes has been used to study histone accumulation during PN development (Fulka *et al.* 2008).

In ICSI, the fertilization steps of capacitation, acrosome reaction and membrane fusion are bypassed. Sperm chromatin enters the ooplasm along with the perinuclear material, acrosome and cell membrane. Eventually, these cellular structures disintegrate inside the oocyte. It has been suggested that they may interfere with sperm chromatin remodeling (Sutovsky *et al.* 1996, Terada *et al.* 2000, Katayama *et al.* 2002, Ajduk *et al.* 2006). Regardless, live offspring have been born using ICSI in a variety of species, including humans and mice (Yanagimachi 2005). However, existing reports on higher incidence of CHR aberrations (Van Steirteghem *et al.* 2002) and lower developmental potential (Morozumi & Yanagimachi 2005, Seita *et al.* 2009) in embryos produced by

ICSI indicate that further evaluations on the effects of the incorporation of the acrosome into the oocyte are needed.

Due to the inability to conduct studies with human embryos, adequate model systems are necessary to study this feature of Hsp CHR transformation during the early events of fertilization. Dynamics of sperm nuclei transformation after heterologous ICSI have not been surveyed so far for any sperm-oocyte pair. Based on the data above (Chapter II), in the present study mPN development with interspecies ICSI utilizing HO injected with Hsp was explored. The detailed kinetics of mPN decondensation using acrosome intact (AI) and acrosome depleted (AD) sperm was established. Heterogeneity in mPN decondensation possibly reflecting intrinsic heterogeneity in the sperm chromatin/nuclear population was demonstrated.

MATERIALS AND METHODS

Preparation of sperm for ICSI

Semen samples were prepared as reported previously (Chapter II). Briefly, after liquefaction, the semen sample was washed with mHTF (Irvine Scientific) supplemented with 0.3% BSA (Sigma). The spermatozoa were washed twice with mHTF–BSA and centrifuged for 10 min at 300g. After the second wash, the supernatant was removed and the pellet was resuspended in fresh mHTF–BSA. Next, washed sperm cells were treated with 1 mM MitoTracker green FM (Molecular Probes) for 15 min at 37°C for visualization of the sperm tail in subsequent microscopy. After MitoTracker treatment, the plasma membranes from sperm cells were removed using 0.5% Triton X-100 (TX) (Sigma) prepared in PBS (Sigma) to generate AD sperm. The cell suspension was vortexed for 1 min then sperm cells were washed in mHTF-BSA three more times prior

to being used for ICSI. Washed sperm without TX treatment were used as the control-AI sperm.

Evaluation of acrosomal membrane status

Acrosomal membrane staining was performed according to the procedure previously described (Fazeli *et al.* 1997) with some modifications. In brief, the sperm samples treated with TX and those serving as control samples were smeared onto microscope slides, air dried, and fixed with absolute methanol. Fixed sperm cells were treated with 100 µg/ml FITC-labeled peanut agglutinin (FITC-PNA) (Sigma) in PBS at 37°C for 30 min. After washing with PBS, the samples were mounted with Vectashield containing DAPI (Vector Laboratories) and then evaluated using a fluorescence microscope (Leitz Ortholux).

Oocyte preparation and ICSI

Frozen HO (Conception Technologies) were thawed and washed for 10 min in mHTF-SSS (Irvine Scientific) at room temperature before being placed into P1 medium (Irvine Scientific) supplemented with 10% SSS. Viable oocytes (97%), as assessed by morphology, were incubated at 37°C in 5% CO_2 prior the ICSI procedure.

ICSI was carried out as previously described (Palermo *et al.* 1992, Chapter II). Briefly, 1 µl of sperm suspension was diluted with 4 µl of 10% PVP (Irvine Scientific) and placed in the center of an injection dish. Each frozen-thawed mature (metaphase II) HO was placed in 5 µl of mHTF-SSS surrounding the central drop containing the sperm suspension and covered with mineral oil. At least 50 metaphase II HO were microinjected for each experimental time (total n = 502 injected oocytes; at least 3 replicates per time point) using Narishige micromanipulators (Narishige) mounted on a phase-contrast

inverted microscope (Olympus) at 400x magnification. The injected oocytes were kept at 37°C in 5% CO_2 for 4, 8, 12, and 16 hr in P1 medium with 10% SSS. After the respective incubation times, degenerate zygotes (swollen or dark) were discarded and viable oocytes were immediately fixed with 2% paraformaldehyde (Sigma) and analyzed for sperm nuclear area.

Microscopy and data analysis

HO were mounted using Vectashield containing DAPI. Total nuclear DNA was visualized on a fluorescence microscope (Leitz Ortholux) using selective or triple-band pass filters and the oil immersion 60 X 1.4 numerical aperture objective. Images were collected using a MagnaFire digital color camera and MicroFire software (Optronics) and processed using Image J software (National Institute of Mental Health, Bethesda, Maryland, USA). Approximately 50 nuclei were observed for each time point post ICSI for both groups. Sperm samples from the TX treated and control groups were also analyzed for nuclear area size (0 hr reference point).

Male pronuclei decondensation was evaluated after staining with DAPI. The surface area of mPN was measured using Image J. Areas of sperm/mPN were evaluated on the analyzer screen. After interactive demarcation of the circumference of the nuclei, the surface areas were automatically calculated by utilizing the enclosed pixels areas. Statistical analysis of nuclear size was conducted using Microsoft Office Excel 2003 (Microsoft, Bellevue, WA, USA). Data were compared by Student's T-test, Mann-Whitney U test or Chi-Square using Sigma Plot 11 (Systat Software, Inc., San Jose, CA, USA).

RESULTS

Two categories of sperm were used for ICSI: AI (control) and AD sperm. To obtain AD sperm, acrosome components were removed by TX. To evaluate acrosome status, sperm staining with FITC-PNA was used. As expected, AI sperm displayed

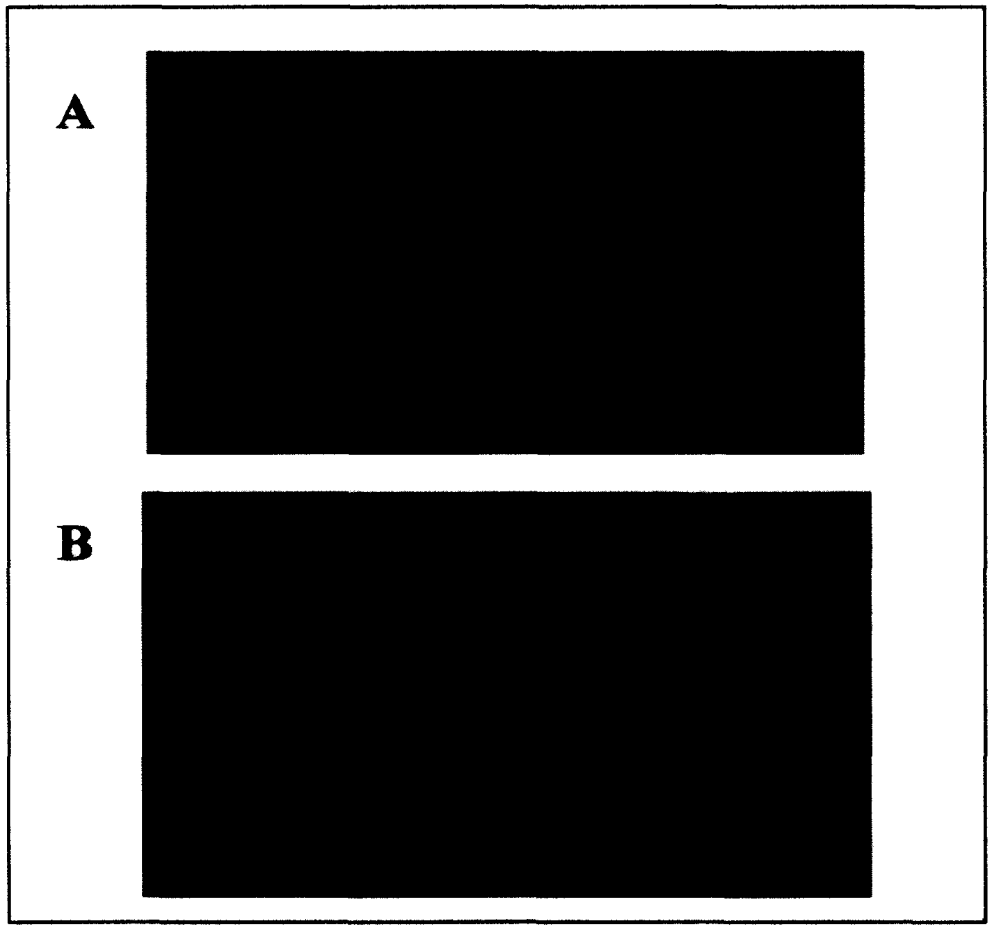

Figure 12 Acrosomal status of human sperm as revealed by PNA staining (FITC-PNA: green). (A) Acrosome intact (AI) sperm, note intense fluorescence of the acrosomal cap. (B) Sperm treated with TX showing weak or no fluorescence were considered as acrosome depleted (AD). Scale bar = 10 μm.

intense fluorescence of the acrosomal cap resulting from PNA binding indicating an intact outer membrane (Fig. 12A). In AD sperm, no fluorescence in the acrosome area was observed indicating partial or complete loss of the outer membrane (Fig. 12B). Treatment with TX generated 95.5% of AD cells. In the control sperm, 12% of cells were lacking acrosome due to damage acquired during sperm processing. The difference between the groups was statistically significant ($p < 0.0001$). Heterologous ICSI resulted in production of 82.9% viable zygotes as assessed by morphology. Male pronuclear decondensation (mPN were identified by tail staining with Mitotracker) was observed in 252 of the 417 (60.2%) viable oocytes. Following ICSI into HO, Hsp decondensed in a time-dependent manner as illustrated by DNA staining with DAPI (Fig. 13A).

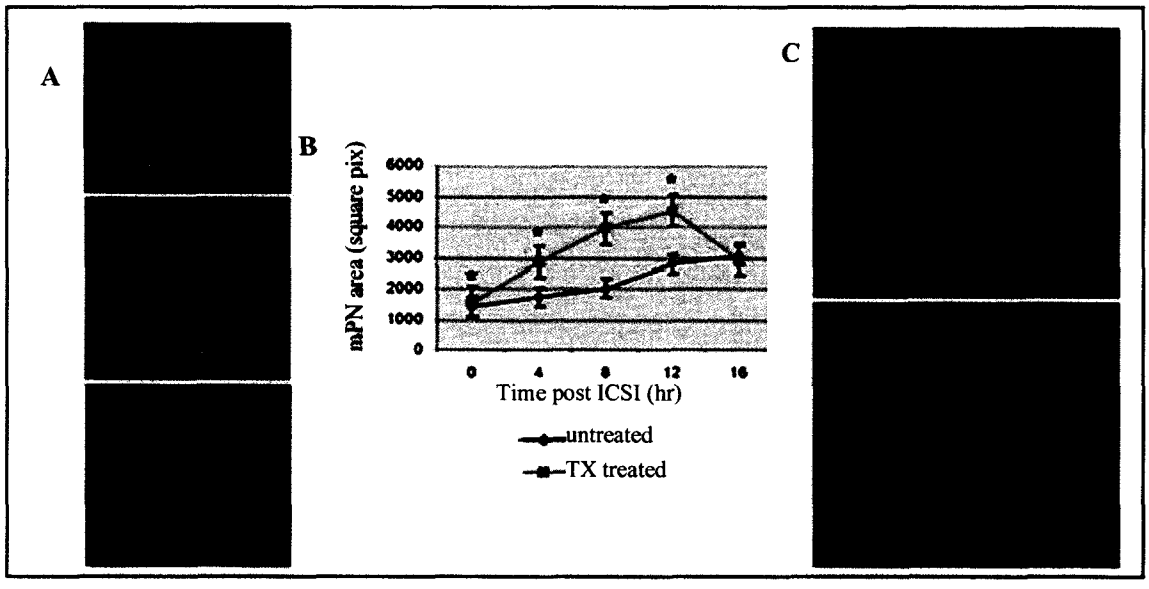

Figure 13 Transformations of human sperm nuclei in hamster oocytes following heterologous ICSI. (A) Typical images of nuclear decondensation of AD sperm cells. (B) Mean nuclear area for TX treated and control spermatozoa. Y-error bars indicate S.E.M.; * indicates significant difference ($p < 0.05$). (C) mPN formation with AI sperm often results in abnormal nuclear decondensation. Total nuclear DNA stained with DAPI (blue) and sperm tail stained with Mitotracker (green). Scale bar = 10 μm.

Progressive mPN swelling was observed in both the AD and AI groups. Fig. 13B shows that Hsp treated with TX decondense more rapidly and with a larger mPN area than the control sperm at 0, 4, 8 and 12 hr post ICSI ($p < 0.05$). PN area gradually increased with swelling reaching a maximum at 12 hr for AD sperm (4540 $\pm$ 387 square pix). Thereafter, the nuclei shrunk to dimensions similar to the 4 hr time point (2651 $\pm$ 475 square pix). At 12 hr post ICSI, the average area of AD mPN (4540 $\pm$ 387 square pix) was three times greater than in sperm at the 0 hr timepoint (1559 $\pm$ 26 square pix). Maximal value of AI mPN area (3074 $\pm$ 328 square pix) was only twice greater than in sperm at 0hr (1430 $\pm$ 387 square pix). Table 2 shows the mean nuclear area for each group and time point post ICSI.

Table 2 mPN area of AD (TX treated) and AI (control) sperm at different time points post heterologous ICSI.

Time	Triton-Treated (AI)	Control (AD)	p value
0 hr	1559 $\pm$ 26	1430 $\pm$ 39	($p = 0.007$)
4 hr	2868 $\pm$ 224	1748 $\pm$ 233	($p < 0.001$)
8 hr	3942 $\pm$ 517	2017 $\pm$ 170	($p = 0.002$)
12 hr	4540 $\pm$ 387	2808 $\pm$ 257	($p = 0.003$)
16 hr	2651 $\pm$ 475	3074 $\pm$ 328	NS

Note: Values are mean $\pm$SEM; area measured in pixels^2.

Some AI mPN demonstrated uneven nuclei decondensation; apparently retention of the acrosome resulted in more condensed DNA in subacrosomal part of PN (Fig. 13C). The

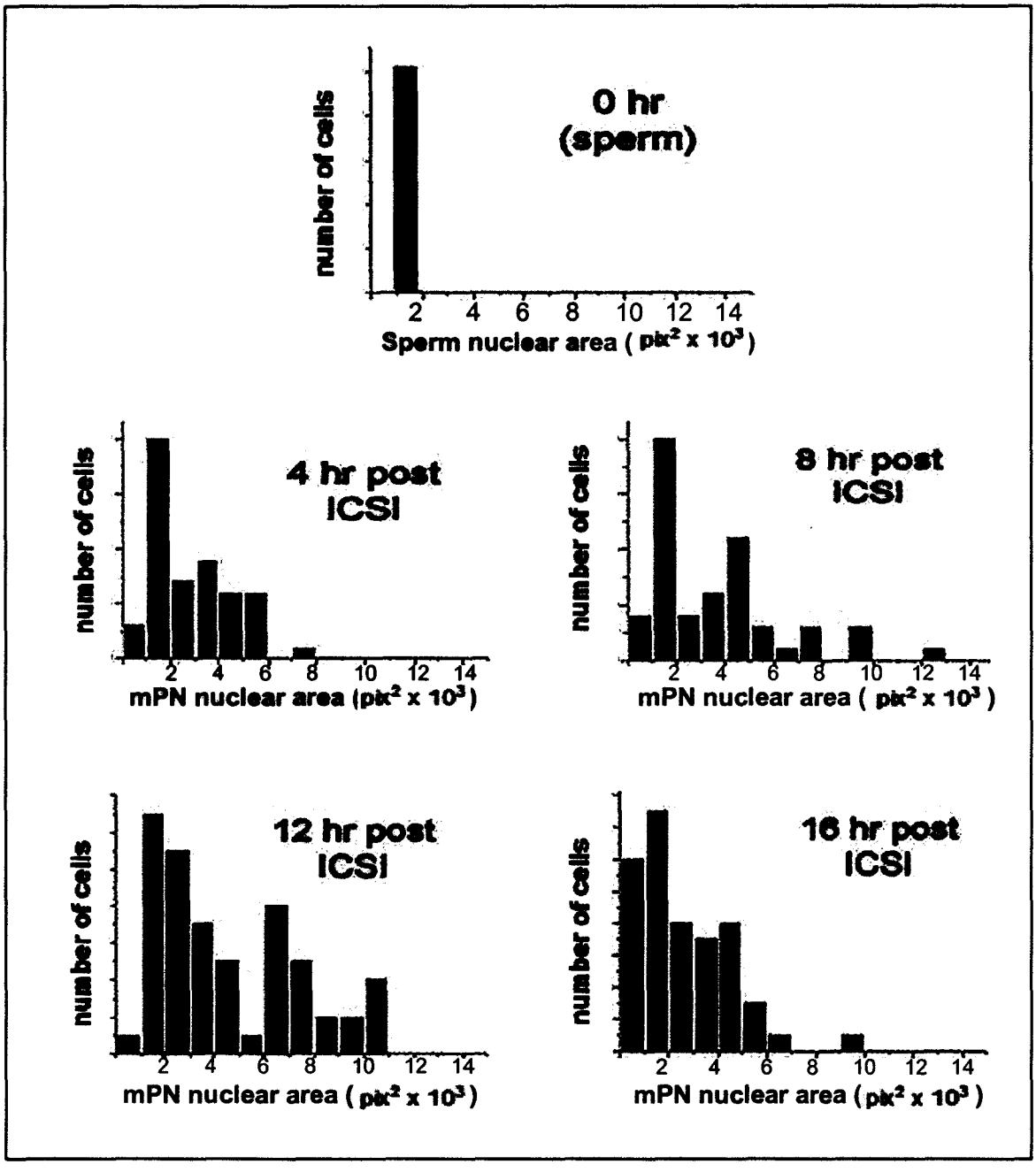

Figure 14 Frequency distribution of mean mPN area (square pixels) demonstrates heterogeneity of sperm population (AD cells).

size of the mPN varied in a collection of zygotes fixed at any time. Indeed, this variability is clearly seen from the frequency distribution of mean nuclear area for AD sperm (Fig. 14). Noticeably, heterogeneity in mPN size was observed at all studied times. This was true for both AD (Fig. 14) and AI (data not shown) sperm. At any time point, some zygotes do not show mPN development. In accordance with Fig. 13B, a fraction of zygotes with highly decondensed mPN reaches a maximum at 12 hr.

DISCUSSION

The ability of spermatozoa to fertilize oocytes depends on a sequence of events ending ultimately in the remodeling of the sperm chromatin from supercompact state packed by PRMs to a relaxed nucleosomal structure. The present study examined Hsp nuclei following ICSI into HO. Four hours post ICSI, developing human mPN was already more decondensed than "native" sperm (0 hr reference point). Decondensation of human mPN progressed in a time-dependent manner in both the AD and AI groups; however, mPN resulting from injection of AD sperm reached a maximum mean area at 12 hr post injection after which time they shrunk to dimensions similar to 4 hr post ICSI Fig. 13B). During natural fertilization, after entry into the ooplasm, sperm chromatin initially becomes partially decondensed and then transiently recondenses into a smaller mass (McLay & Clarke 2003). Apparently, this feature was reflected in the current heterologous ICSI approach. Similar decondensation/recondensation was observed in our preliminary study using the incubation of Hsp in XEE (Chapter I, Mudrak *et al.* 2009). Within a given sample of spermatozoa, variations in mPN development as judged by nuclear area size were observed (Fig. 14). This may reflect the intrinsic heterogeneity in the mature nuclear Hsp population. One of the possible reasons for such variation may be

due to the sperm-specific histone TSH2B (Van Roijen *et al.* 1998, Zalensky *et al.* 2002). This histone is present in only a 30% subpopulation of sperm cells. Significant correlation between TSH2B level and Chromomycin A3 staining of individual spermatozoa resulting from loosened packaging of DNA has been demonstrated (Singleton *et al.* 2007). In studies using the XEE model, sperm cells containing TSH2B decondensed more rapidly and to a greater extent than did spermatozoa without this histone (Singleton *et al.* 2007). Other possible reasons for size heterogeneity of mPN may include sperm DNA damage, cell to cell variability in sperm DNA methylation, heterogeneity of oocytes or DNA replication in the mPN.

One of the major differences between natural fertilization and ICSI is the absence of sperm modification which naturally occurs during sperm passage through cumulus cells, zona pellucida and oolemma (Yanagimachi 1994). Typically, AI sperm are used for the ICSI procedure. In the present study both AI and AD sperm were used. In AD sperm, the acrosome was completely removed (Fig. 12B). Importantly, sperm treated with the non-ionic detergent TX, used for solubilizing membrane proteins, developed mPN at a more advanced rate with larger mean nuclear area than non treated sperm (Fig. 13B). Similarly, in homologous rat ICSI, the timing of PN formation using TX or lysolecithin treated sperm was significantly accelerated compared to control sperm (Seita *et al.* 2009). In the mouse, homologous ICSI of TX treated sperm yielded no difference in fertilization, blastocyst, implantation and live birth rates compared to control sperm (Ahmadi & Ng 1997). These reports indicate that sperm pre-treatment may be used in clinical ICSI; however more studies in this direction are needed to prove its safety.

It has been proposed that the ICSI procedure possibly causes an overall delay in mPN development and paternal genome activation with individual sperm CHRs differentially affected. Indeed, in Hsp, CHRs occupy preferred, defined intranuclear positions (Zalenskaya & Zalensky 2004, Mudrak *et al.* 2005, Manvelyan *et al.* 2008). Paternal genome is activated early after fertilization, during S/G2 phase of the first cell cycle i.e. before syngamy (Adenot *et al.* 1997). Therefore, specific CHR positioning in sperm may determine their non-random and ordered activation (Schultz & Worrad 1995, McLay & Clarke 2003, Zalensky & Zalenskaya 2007). An increased rate of sex chromosomal anomalies has been reported in human babies conceived by ICSI (Bonduelle *et al.* 2002). This increase could be due to the fact that the sex CHR X was found to be preferentially localized at the subacrosomal region of the sperm (Luetjens *et al.* 1999, Hazzouri *et al.* 2000, Zalenskaya & Zalensky 2004). It may be suggested that these anomalies, at least in part, are connected with delayed CHR processing of sperm CHRs residing in the apical tip (Luetjens *et al.* 1999). Furthermore, preservation of intact acrosome during ICSI most probably is the major cause of delayed or hindered decondensation of the apical region of the sperm during PN development (see example Fig. 13C).

In conclusion, the kinetics of Hsp nuclei transformation under the influence of ooplasm in a heterologous ICSI model was demonstrated. The influence of acrosome preservation on sperm DNA decondensation was illustrated. These findings propose that human-hamster ICSI mimics major events that occur during natural fertilization in humans. Due to the impossibility to use homologous human ICSI for research, the

heterologous ICSI approach, as described here, may be an effective approach to study processing of individual sperm CHRs/chromosomal domains during mPN development.

CHAPTER IV

PROTAMINE WITHDRAWAL FROM HUMAN SPERM NUCLEI FOLLOWING HETEROLOGOUS ICSI INTO HAMSTER OOCYTES

INTRODUCTION

The major function of sperm is to safely transfer genetic and epigenetic information to the future zygote in the state appropriate for its programmed activation. Spermatozoa are unique among all other cell types and are the product of the multistep and complex process of spermatogenesis. This process is characterized by unprecedented genome reorganization and morphological restructuring of the differentiating male germ cells. In particular, dramatic nuclear remodeling is accomplished during the late stages of spermatogenesis (spermiogenesis) when a stepwise transformation of nucleosome-based chromatin into sperm-specific nucleoprotamine takes place [reviewed in (Wouters-Tyrou *et al.* 1998, Lewis *et al.* 2003)]. This exchange leads to the highest degree of DNA compaction known in eukaryotes (Ward & Coffey 1991). In humans, two types of highly basic chromosomal proteins - human protamine (Hup) 1 and Hup 2 are present in sperm nuclei (Balhorn et al. 1999, Braun 2001, Oliva 2006, Balhorn 2007) and it has been shown that both are essential for normal sperm function (Cho *et al.* 2001).

After penetration of spermatozoa into oocytes, sperm chromatin is remodeled to a somatic type, before DNA replication and the subsequent preparation for first mitosis to complete fertilization (Perreault 1992, McLay & Clarke 2003). Supposedly, sperm chromatin reorganization in ooplasm coincides with cytologically observed decondensation and formation of mPN. At the molecular level, the removal of PRMs

and their replacement with maternally provided histones is believed to be a two-step process: physical removal or degradation of PRM (Yanagimachi 1994, Sutovsky & Schatten 1997) followed by assembly of mPN chromatin into nucleosomes (McLay & Clarke 2003, Poccia & Collas 1996). It is proposed that sperm chromatin remodeling in the zygote depends on multiple oocyte activities such as glutathione reduction of PRM disulfide bonds (Perreault *et al.* 1988, Sutovsky & Schatten 1997), or trafficking by nucleoplasmin-like proteins (Burns *et al.* 2003, Frehlick *et al.* 2007). However, these activities remain largely unknown and even straightforward information concerning the timing of PRM removal after sperm penetration into ooplasm is limited to several publications. In early studies of mouse fertilization, Rodman (Rodman *et al.* 1981) showed early disappearance of PRM while Nonchev and Tsanev (1990) found that these proteins were still present in mPN 8 hr after sperm penetration. Both studies used immunolocalization of PRM in zygotes. In any case, PRM were replaced by histones before the onset of DNA replication (Nonchev & Tsanev 1990). In fertilized pig oocytes resulting from IVF, PRM dissociation studied using immunohistochemistry was registered just after sperm penetration, before nuclear decondensation and mPN formation (Shimada *et al.* 2000, Nakazawa *et al.* 2002, Kikuchi *et al.* 2006). In summary, limited amount of data obtained using different techniques of PRM detection and animal models allow only limited conclusions on the timing of PRM-histone transition in the developing zygote.

Here, the removal of human PRMs Hup 1 and Hup 2 using immunofluorescent localization following heterologous ICSI of Hsp into HO was described. Human-hamster ICSI, a robust and well-established system (Yanagida *et al.* 1991, Jones *et al.* 2010), was

chosen due to inability to conduct studies involving formation of human zygotes. Removal of both PRMs from mPN occurred within 1 hr post ICSI and was correlated with the extent of PN decondensation/development.

MATERIALS AND METHODS

Human spermatozoa preparation

Semen samples were prepared as previously described (Chapters II, III). Briefly, after liquefaction, the semen sample was thoroughly washed with mHTF-BSA. After the final wash, plasma and acrosomal membranes were removed from sperm cells using 1 min treatment with 0.5% TX (Sigma) prepared in PBS (Sigma). Sperm cells were washed from TX in mHTF-BSA prior to being used for ICSI. In some experiments spermatozoa were stained with 1 mM MitoTracker green FM (Molecular Probes) for 15 min at 37°C for visualization of the tail in subsequent microscopy.

Oocyte preparation, ICSI and zygote preparation

For heterologous ICSI frozen HO from Conception Technologies (San Diego) were used. Preparation of oocytes for injection has been described in detail (Jones *et al.* 2010) and only viable oocytes (97%) were used.

ICSI was carried out as described (Palermo *et al.* 1992, Jones *et al.* 2010). Briefly, 1 µl of sperm suspension was diluted with 4 µl of 10% PVP (Irvine Scientific) and placed in the center of an injection dish. Each frozen-thawed mature (metaphase II) HO was placed in 5 µl of mHTF-SSS surrounding the central drop containing the sperm suspension and covered with mineral oil. At least 30 metaphase II HO were microinjected for each experimental time (total n = 134 injected oocytes; at least 2 replicates per time

point). Sperm were randomly selected with no strict morphological criteria for injection into recipient HO. The injected oocytes were kept at 37°C in 5% CO_2 for 0, 0.5, 1 and 12 hr in P1 medium (Irvine Scientific) with 10% SSS. Prior to fixation of the zygotes, the zona pellucida was removed with acidic Tyrode's solution (pH 2.5). Viable zygotes were fixed at respective times post ICSI with 2% paraformaldehyde (Sigma) for 45 min, washed in PBS/0.2% Tween-20 (Sigma) and stored at 4°C until use.

Immunofluorescent localization of protamines

The specificity of immunofluorescent localization reaction using anti-PRM antibodies (mouse monoclonal anti-Hup 1M and Hup 2B; SHAL Technologies, Inc., Livermore, CA, USA) was evaluated using sperm cells fixed with 1% paraformaldehyde for 1 min, washed with PBS, and then decondensed in a 0.1 mg/ml heparin, 20mM DTT in PBS for 30 min at RT. Partially decondensed cells were loaded onto microscopy slides and dehydrated with a series of alcohols. The cells were permeabilized in cold (-20°C) ethanol for 30 min then air dried. Slides were blocked in a Blocking buffer (3% BSA, PBS, 0.1% Tween-20) for 30 min at RT. Then primary antibodies were applied at a dilution of 1:100 and incubated for 2 hr at 37°C. After washings in PBS Alexa Fluor 594 goat anti-mouse IgG (Molecular Probes, Eugene, Oregon, USA) was applied at a dilution of 1:1000 and incubated for 45 min at 37°C. Finally, slides were mounted using Vectashield (Vector Laboratories) containing DAPI. Slides on which primary antibody staining was omitted were used as a negative control.

For PRM localization in zygotes, the fixed zygotes were incubated in 0.5% TX in PBS for 30 min at RT prior to blocking. Zygotes were then blocked with 3% BSA, 0.1% TX, 5 mM DTT in PBS for 40 min at RT. Zygotes were then washed extensively in PBS

containing 0.1% TX, 1% BSA. To detect PRM the monoclonal antibodies against Hup 1 and Hup 2 were used at a dilution of 1:100 and incubated for 90 min at 37°C. After washing primary antibodies were detected using Alexa Fluor 488 goat anti-mouse IgG (Molecular Probes) at a dilution of 1:1,000 and incubated for 60 min at 37°C. Slides were mounted with Vectashield containing DAPI or propidium iodide (PI).

Image capture and analysis

Immunostaining results were visualized using a Leitz Ortholux microscope with an oil immersion objective 60×, 1.4NA. Triple band-pass filter set was used for simultaneous visualization of green, red and blue fluorescence. Images were collected using a MagnaFire digital color camera and MicroFire software (Optronics Inc). Images were processed in Adobe Photoshop 7.0 (Adobe Systems).

Male pronuclei decondensation was evaluated after DNA staining with DAPI or PI. The surface area of mPN was measured using Image J. Areas of sperm/mPN were evaluated on the analyzer screen. After interactive demarcation of the circumference of the nuclei, the surface areas were automatically calculated by utilizing the enclosed pixels areas.

RESULTS

Visualization of protamines in sperm

To check the specificity of the immunolocalization reaction and to adjust working concentrations and conditions of immunofluorescence, localization of Hup1 and Hup2 in Hsp was first performed. The dense structure of chromatin does not allow antibody penetration; therefore, controlled swelling of cells with Heparin/DTT was used as described in (Zalensky *et al.* 1993), see Methods for details. Staining of decondensed

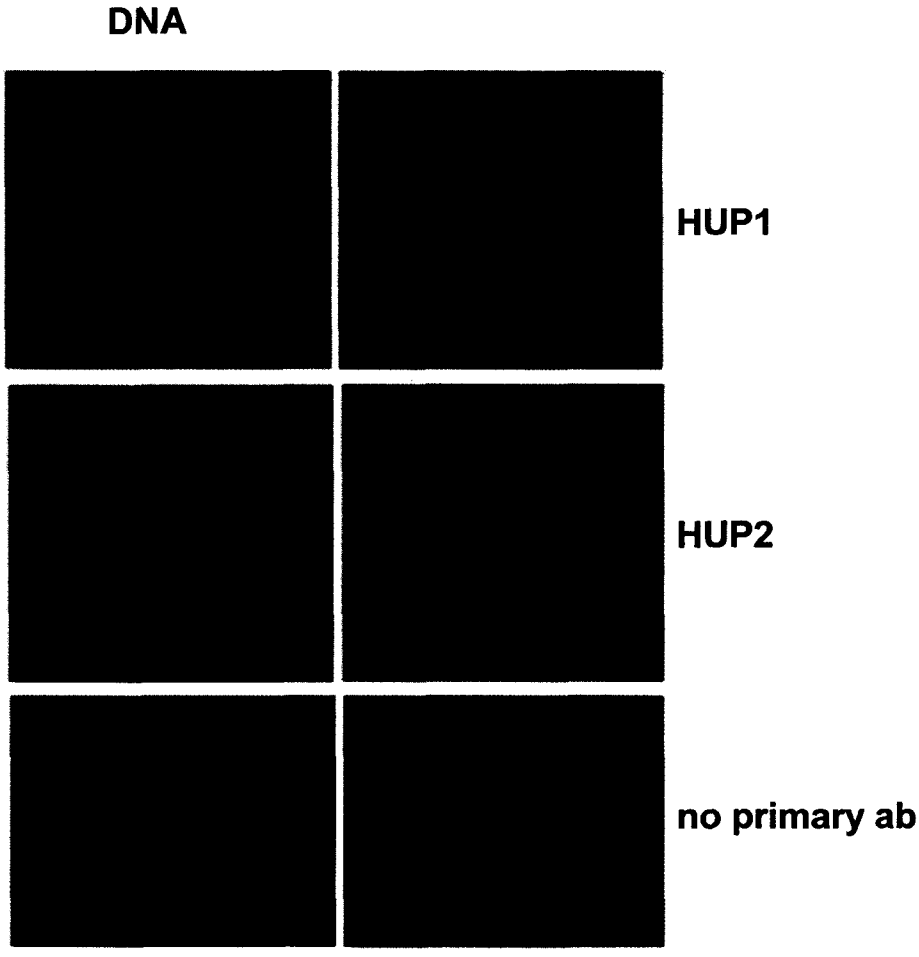

Figure 15 Visualization of P1 and P2 in human sperm Human sperm were partially decondensed in vitro and stained with anti-Hup1 (top panel) and anti-Hup2 (middle panel). Nuclear DNA counterstained with propidium iodide. Control (bottom panel) demonstrates specificity of detection.

sperm with both antibodies showed relatively homogeneous PRM distribution coinciding with DNA localization (Fig. 15). In the absence of primary antibodies (Fig. 15, bottom right panel) staining was absent demonstrating specificity of localization.

Heterogeneity of human male pronuclei formation in heterologous ICSI

At any time point post ICSI noticeable variations in nuclear size of the developing mPN as revealed by DNA staining (Fig. 16A) were observed. Similar type of variability at different times from 15 min to 1 hr and at intervals up to 16 hr has been observed in our earlier study (Jones et al. 2010). More detailed analysis demonstrated extremely broad distribution in median sizes of mPN nuclei areas (NA) as determined from DNA staining. The NA in the "most developed" mPN exceeds that of intact sperm 10 times. For convenience of analysis all PN imaged for PRM presence (totally 127 zygotes for three time points studied; at least 2 replicates per time point) were grouped into three categories according to NA measured in PN stained for DNA: compact - 480 pixels^2, median NA (40% of zygotes); decondensing - 1060 pixels^2, (40%); and decondensed - 2,700÷5,000 pixels^2 (20%). The percentage of decondensed PN increases from 30% at 15 min up to 70% at 60 min.

Protamine dissociation from sperm nuclei

To determine the mode and dynamics of PRM removal, immunolocalization of Hup1 and Hup2 in hybrid zygotes was performed at 15 min, 30 min and 1 hr post ICSI with representative images shown in Fig. 16 B-D. The character of PRM localization correlated with mPN size rather than with the time post ICSI when the zygote had been fixed. The character of PRM immunofluorescence was analyzed in three size groups of pronuclei NA (see above). In compact mPN, staining for PRM was not detected as shown

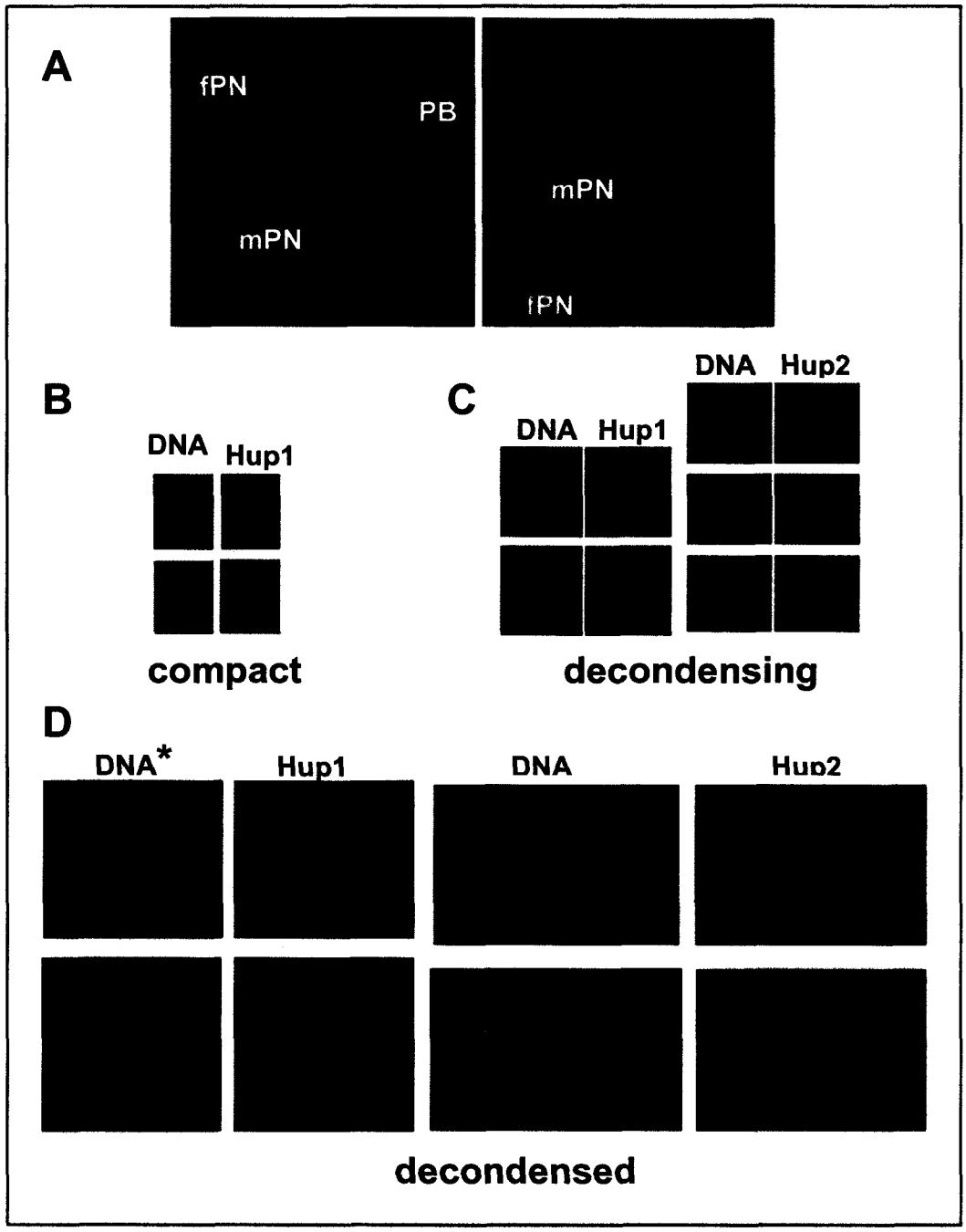

Figure 16. Dissociation of PRM from human sperm following heterologous (human sperm-hamster oocytes) ICSI. (A) Typical images illustrating variations in human sperm processing in hybrid zygote. Left panel – **compact, right panel – decondensed male pronuclei at 1 hr post ICSI. Total nuclear DNA** stained with DAPI (blue) and sperm tail stained with Mitotracker (green). (B-D)Representative images of human protamines immunolocalization in compact mPN (B), in decondensing mPN (C), and decondensed mPN (D). Cut-outs from whole zygote images similar to that shown in Fig. 16A, but stained both for DNA (blue) and protamines (green).

for Hup 1 (Fig. 16B), or observed as a weak staining on the nucleus rim (not shown). Most likely, similarly to non-treated sperm, PRM epitopes in the compact PN are not accessible to antibodies. Fig. 16C illustrates typical patterns observed in decondensing mPN. Noticeably, these PN demonstrated areas of more compact DNA characterized by intense staining with DAPI surrounded by spreading chromatin (Fig. 16C left panels). At this stage, both Hup 1 and Hup 2 are largely detected in the region of the decondensing peripherally located chromatin while the compact internal area showed almost no reaction with antibodies. In decondensed mPN, Hup 1 was completely absent, while trace amounts of Hup 2 were still observed (Fig. 16D), which may indicate slightly different kinetics of both PRMs removal from sperm.

DISCUSSION

Using immunofluorescence with antibodies against human PRM applied to the transforming human spermatozoa injected into HO, the disappearance of these proteins in the process of hybrid zygote development was analyzed. Both PRMs (Hup 1 and Hup 2) are completely withdrawn from mPN when the area of its nuclei increases 6-10 times over the sperm NA. Importantly, very high heterogeneity observed in mPN development within the zygotes precluded identification of the uniform post ICSI time of PRM removal. Indeed, significant variations in mPN size were observed at any time after fertilization studied (15, 30, and 60 min.). In Chapter III, similar heterogeneity in the degrees of sperm transformation at multiple time points, up to 16 hr post ICSI was demonstrated (Jones *et al.* 2010). In summary, this data clearly demonstrated zygote to zygote variation in human mPN development at all times post injection studied. Some male gametes stay in non-processed compact state while others undergo nuclear

decondensation and apparently chromatin transformation with different speed. Such individual diversity in zygote development does not allow assigning time post ICSI when PRMs completely disappear from human mPN.

Up to now, removal of PRM from mammalian sperm following fertilization has been explored in a small number of publications. Several studies have been performed using mouse fertilization. Rodman *et al.* (1981) using immunofluorescence with the antiserum to sperm nuclear basic proteins (SNBP) reported that these proteins (which include PRM) are displaced very soon after sperm entry. In contrast, Nonchev and Tsanev (1990) reported that PRM were still present in mPN 8 hr after sperm penetration and their loss occurred as histones appeared in the well-developed PN before the onset of DNA replication. More recently, Van der Heijden *et al.* (2005) found that mouse PRM removal from expanding chromatin was completed at 30 min after gamete fusion. Therefore, it is difficult to unambiguously assign a time frame for PRM to histone exchange during fertilization in mice which in the cited publications varied from minutes to 8 hr. The only other mammal studied was pig. Using IVF of pig oocytes and immunohistochemistry with anti-PRM antibodies, it was shown that PRM removal occurred just after sperm penetration and before sperm decondensation and mPN formation (Shimada *et al.* 2000, Nakazawa *et al.* 2002, Kikuchi *et al.* 2006). Shimada *et al.* (2000) reported that the proportion of condensed sperm nuclei that reacted with PRM antiserum was 87% at 2 hr post insemination and gradually decreased to 13% at 5 hr after initial insemination (Shimada *et al.* 2000). Unfortunately, all discussed studies lack information about numbers of cells analyzed, and the existence of zygote to zygote

variability in mPN development, which has been previously observed (Chapter III), was not explored in other mammals.

What are the biological reasons for the detected variations in mPN development seen here? They may be a consequence of the heterologous ICSI approach used, although heterogeneity of Hsp is a more probable explanation. Noticeable morphological diversity of Hsp cells in any ejaculate is evident at first glance in routine microscopic examination. It has been known that individual's sperm morphology fluctuates within-subject or among fertile men, with the mean percentage of abnormal forms reaching 50% (Schwartz *et al.* 1986). Variations in sperm size as determined by ratio of head axes were observed in 457 ejaculates from 16 fertile donors (Katz *et al.* 1986). Variability of Hsp population within a given ejaculate may be, at least in part, determined by strikingly uneven distribution of sperm-specific histone TSH2B present in 30% of cells (Zalensky *et al.* 2002, Singleton *et al.* 2007, Singleton *et al.* 2007). Spermatozoa containing TSH2B decondense more rapidly and to a greater extent in XEE (Mudrak *et al.* 2009). Studies regarding mPN development in human zygotes produced by either natural fertilization or ART are absent because of obvious reasons. In the absence of such information and based on the above considerations, the existence of irregular non-uniform development of human zygotes *in vivo* due to male gamete contribution is a likely explanation. This cryptic anomaly of sperm may be one of the reasons for poor early embryonic development and spontaneous abortions.

At early stages (Fig. 16B), PRMs are undetectable by immunofluorescence most probably due to chromatin compaction, which makes their epitopes inaccessible to antibodies. In the early work (Rodman *et al.* 1981), mouse SNBP were localized in the

posterior region of still compact mPN and it was suggested that "unmasking" of antigenic sites occurred first in the basal region of the sperm nucleus. Comparison with our data is unsuitable because of differences in experimental approaches - animal model, type of antibodies and detection techniques. In decondensing PN (Fig. 16C), both Hup 1 and Hup2 were associated largely with the periphery of nuclei and are localized with less condensed chromatin. This is more evident for Hup 2 which is associated with the emerging DNA halo and is completely "absent" in the area of more compact DNA (Fig. 16C right panels). Such localization of the human PRM in decondensing mPN illustrates one fixed stage of their removal promoted by hamster ooplasm. In fully developed (decondensed) mPN both PRM are virtually absent; only trace amounts of Hup2 may be noticed (Fig. 16D, right). It should be stressed once again that mPN demonstrating each type of PRM localization may be found in zygotes fixed at 15, 30, and 60 min post ICSI although the number of decondensed PN increases with time.

In conclusion, in HO, human PRM are removed rather quickly (possibly within 1 hr post ICSI) from those sperm nuclei which decondense and form mPN. More detailed experiments concerning PRM to histone substitution, fate of human sperm-specific histones, and sperm CHR transformation are underway.

CHAPTER V

INTRANUCLEAR POSITIONING OF HUMAN SPERM CHROMOSOMES 18 AND 19

INTRODUCTION

Within the last 10 years, significant developments in the study of nuclear architecture have been reported. Nuclear architecture comprises all elements of the cell nucleus, including the topology of CHR. It has been shown that CHR structure and intranuclear localization play an important role in regulating genome activity (Cremer & Cremer 2001, Claussen 2005, Dehghani *et al.* 2005, Foster & Bridger 2005).

CT localization in the interphase nucleus is largely regarded to be non random. However, the exact nature of this organization and the mechanism for conveying positional information to daughter nuclei are still very controversial (Williams & Fisher 2003). CHRs in interphase are relatively immobile and some authors have demonstrated that global CHR positioning is heritable through cell division (Gerlich *et al.* 2003). Other studies indicated that the positioning is not inherited through mitosis but is established *de novo* during the subsequent interphase stages (Hagstrom & Meyer 2003, Walter *et al.* 2003, Cremer *et al.* 2004, Thomson *et al.* 2004).

The Hsp cell presents advantages for chromosomal localization over the somatic cell: they are relatively flat, asymmetric and have internal spatial markers - acrosome and the tail attachment point. Therefore, the relative positions of CHR can be much more easily defined in the sperm than in the somatic cells. The principal of CHR territorial organization is preserved in sperm cells (Haaf & Ward 1995, Zalensky *et al.* 1995, 2002,

Zalenskaya *et al.* 2000) while the chromatin of sperm CHRs is 4-6 times more condensed than in metaphase CHR (Haaf & Ward 1995, Mudrak *et al.* 2005). Details of the unique genome architecture of human spermatozoa have been discussed in Chapter I.

Because of extended shape of the nucleus, the CHR localization in sperm can be assessed both in the radial and in the longitudinal (along the anterior-posterior axis) direction. In order to determine the longitudinal position of the CHRs, the length of the sperm nucleus was typically divided into equal sectors and the number of FISH signals, corresponding to each sector, was calculated for the CHR analyzed. As a result CHR longitude positioning was termed as "subacrosomal, equatorial or basal" (Sbracia *et al.* 2002) and "anterior, medial or posterior" (Foster *et al.* 2005). Alternatively, distances between the center of FISH signals and the tail attachment point were measured, normalized and served as a characteristic of longitude localization. Radial positioning was determined by CHR distances to the nearest point at nuclear periphery (Foster *et al.* 2005) or to the long axis of the nucleus (Zalenskaya & Zalensky 2004), by number of FISH signals registered within enumerated radial "shells" (Finch *et al.* 2008, Manvelyan *et al.* 2008).

In summary, data from several groups concur in the existence of the distinct CHR localization in human spermatozoa. For example, HSA 6 and 7 are peripheral in location while HSA 16 and X are more internal (Zalenskaya & Zalensky 2004); HSA 2, 5, 6 and 18 have been found in the basal part of the sperm nucleus, while HSA 1, 7 and X - in the apical area (Luetjens *et al.* 1999, Hazzouri *et al.* 2000, Sbracia *et al.* 2002, Zalenskaya & Zalensky 2004, Mudrak *et al.* 2005). A defined, non-random spatial localization of sperm CHR attract interest since it was speculated that CHR positioning may participate

in the determination of sequential expression of the paternal genome after fertilization (Greaves *et al.* 2003, Zalensky & Zalenskaya 2007). In this work, the positioning of two human CHR with similar size but different in gene content - HSA 18 (gene-poor) and HSA 19 (gene-rich) was determined. These characteristics were determined using FISH with painting probes and a novel approach for statistical evaluation/presentation of experimental data.

MATERIALS AND METHODS

Human spermatozoa preparation for FISH

Semen samples were obtained from fertile donors. Sperm were washed three times in 1XPBS (phosphate-buffered saline: 170 mM NaCL, 3.4 mM KCL, 1 mM Na2HPO4, 2 mM KH2PO4, pH 7.2). The pellet was resuspended in PBS and equal volume of 1% formaldehyde was added for fixation. In 1 min a great excess of PBS was added to dilute formaldehyde. Cells were centrifuged and the pellet was resuspendend in 1XPBS. An equal volume of 2X Decondensation solution (40 mM DTT, 0.4 mg/ml heparin) was added. Cells were treated with this 1X Decondensation Solution for 30 min at RT. Sperm cells were then loaded onto microscopic slide in ~ 10 µl of decondensation solution, allowed to sit for 30 min, rinsed with PBS, dehydrated in ethanol series (70%, 80%, 90%, and 100%) and air-dried.

Fluorescent in situ hybridization

Whole painting probes for HSA 18 and 19 were purchased from Starfish (Cambio, Cambridge, UK). HSA 18 was directly labeled with FITC while HSA 19 was

labeled with Biotin. Concentrated paint probes were denatured for 10 min at 75°C and reannealed at 37°C for 45 min to exclude repetitive sequences from hybridizing. Microscopic slides with the cells were denatured in 70% formamide in 2X SSC, for 2 minutes at 75°C, dehydrated in cold ethanol series and air-dried. Probe was applied onto slide. Hybridization was performed under coverslip in wet chamber overnight at 37°C. Post-hybridization washings consisted of two 7-min washes in 50% formamide in 2X SSC at 46°C and two 7 min washes in 4X SSC, 0.2%Tween-20 at 46°C.

To detect Biotin-labeled HSA 19 probes, the cells were blocked in 5% BSA, 2X SSC, 0.1% Tween-20 for 30 min at RT, then avidin-Texas Red (TR; Vector Laboratories, Inc., Burlingame, CA, USA) diluted 1:200 in Blocking Solution was applied on slide. Slides were incubated at 37°C for 1 hr and washed in 3% BSA, 2X SSC, 0.1% Tween-20 three times for 10 min at RT. No amplification was needed for the directly labeled HSA 18 probes. Slides were mounted using Vectashield with DAPI (Vector Laboratories, Inc.).

Image capture and analysis

Hybridization results were visualized using a Leitz Ortholux microscope with an oil immersion objective 60×, 1.4NA. Triple band-pass filter set for simultaneous visualization of FITC, TR and DAPI fluorescence was used; in some cases selective "green" filter was used. Images were collected using a MagnaFire digital color camera and MicroFire software (Optronics Inc). Only nuclei in which chromosome territories were unfolded and had almost round, compact shapes were selected for measurements. CHR localization was characterized by (X, Y) coordinates of CT center, which was

determined using digital images and Sigma Scan Pro (Systat Software, San Jose, California, USA). In more detail, Fig. 17 illustrates measurement scheme used: the length (L) and the width (D) of the sperm nucleus; distance between CT center and the

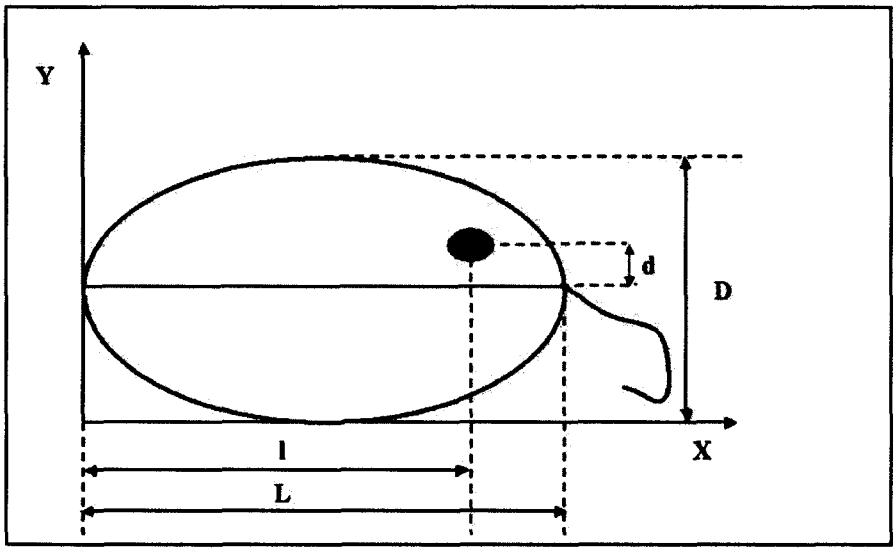

Figure 17 Schematic representation of measurements used to determine coordinates (X, Y) of CT centers (chromosome positioning).

acrosomal end along the Y-axis (l); distance between CT center and the long nuclear axis (d). About 100 sperm cells were analyzed for each chromosome. Statistical analysis was performed in Microsoft Excel. In order to improve accuracy and reduce observer bias, the measurements were performed by two observers independently. Two-tailed T-test for independent groups has shown that the two data sets were not statistically different (the P-value > 0.05). At the final step coordinates of CTs (X=l; Y=0.5D±d) were normalized

to account for differences in nuclear swelling for individual cells and introduced into Origin 6.0 software to generate the histograms and contour plots for each chromosome.

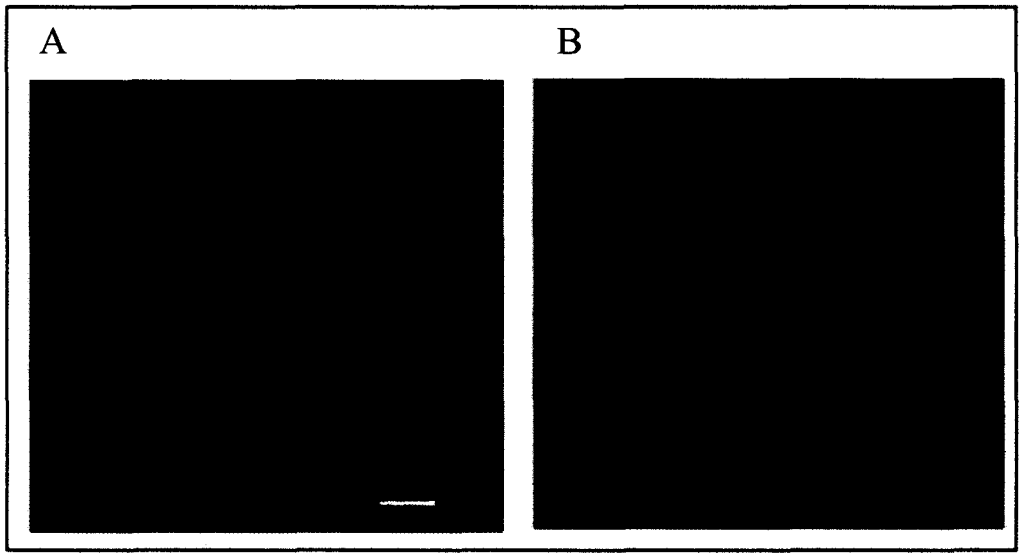

Figure 18 Representative FISH with whole chromosome paining probes. (A) HSA 18, directly labeled with FITC (green), no DNA counterstaining. (B) HSA 19, labeled with Biotin and detected with Avidin-TR, total DNA counterstained with DAPI (Blue). Scale bar 10 μm.

RESULTS

In this study the localization of two chromosomes HSA 18 and 19 in sperm nuclei was determined. First, CTs were imaged using FISH as illustrated (Fig. 18), then coordinates of each CT center were determined as described in Methods. Preferred radial and longitude positioning were determined from the contour plots and the histograms. Figs. 19 and 20 show final results of positioning analysis of HSA 18 and HSA 19 in spermatozoa.

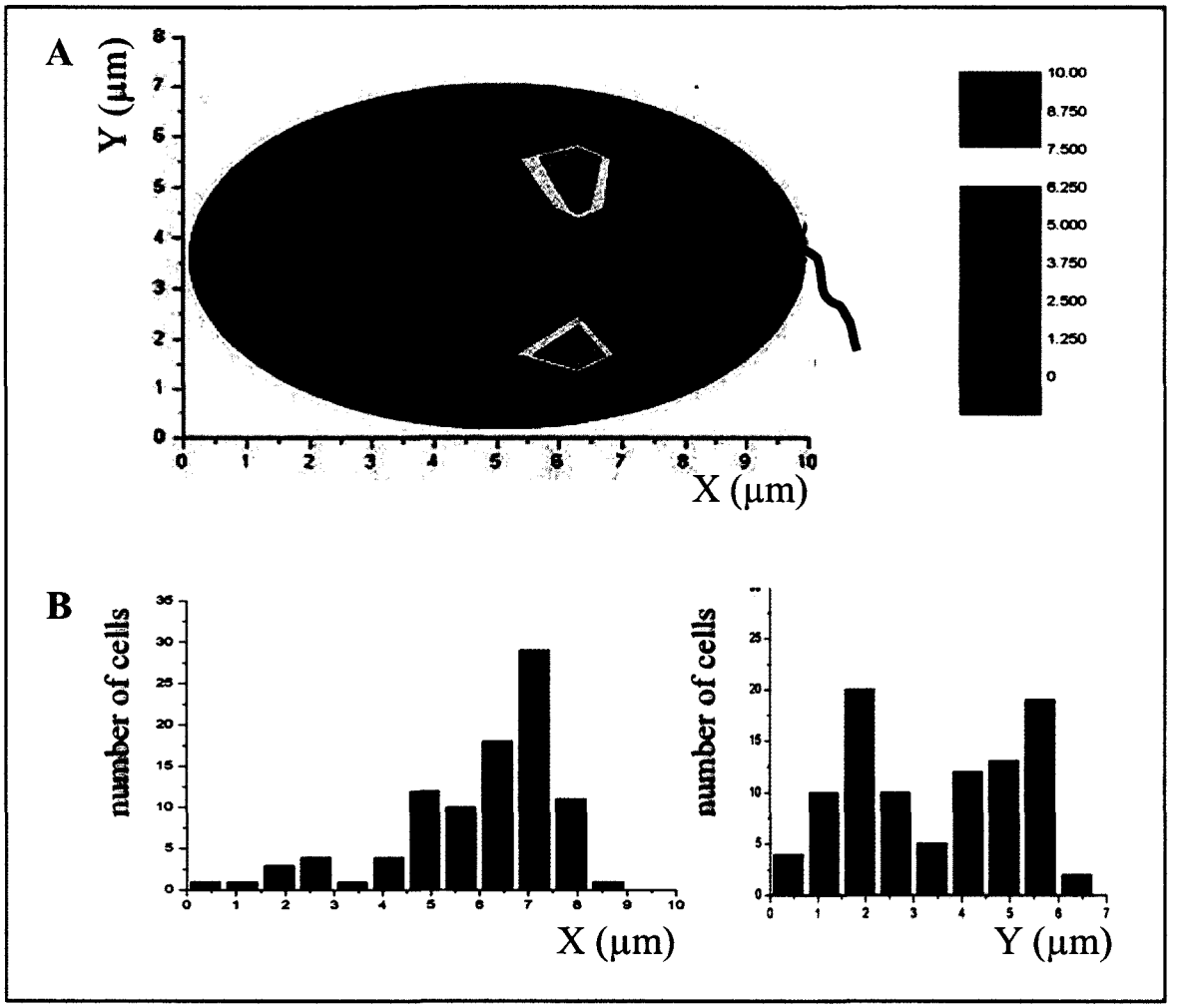

Figure 19 Intranuclear positioning of HSA 18 in human spermatozoa. (A) Plot of CT centers distribution showing probability values, red color-highest probability. (B) Frequency distribution of CT centers longitude (x) and radial (y) localization.

The color filled contour plots in Figs. 19 and 20 (A) represent the longitudinal (along x-axis) and radial (along y-axis) distribution of CT centers in sperm nuclei. Contour plots (parts A in Figs. 19, 20) show probabilities of finding CT with (X, Y) coordinates in 2D space representing sperm nuclear area. Colors correspond to frequencies of the experimentally observed (X, Y) (red - the highest, blue - the lowest).

The X and Y histograms (parts B in Figs. 19 and 20) were constructed using the same sets of raw data and

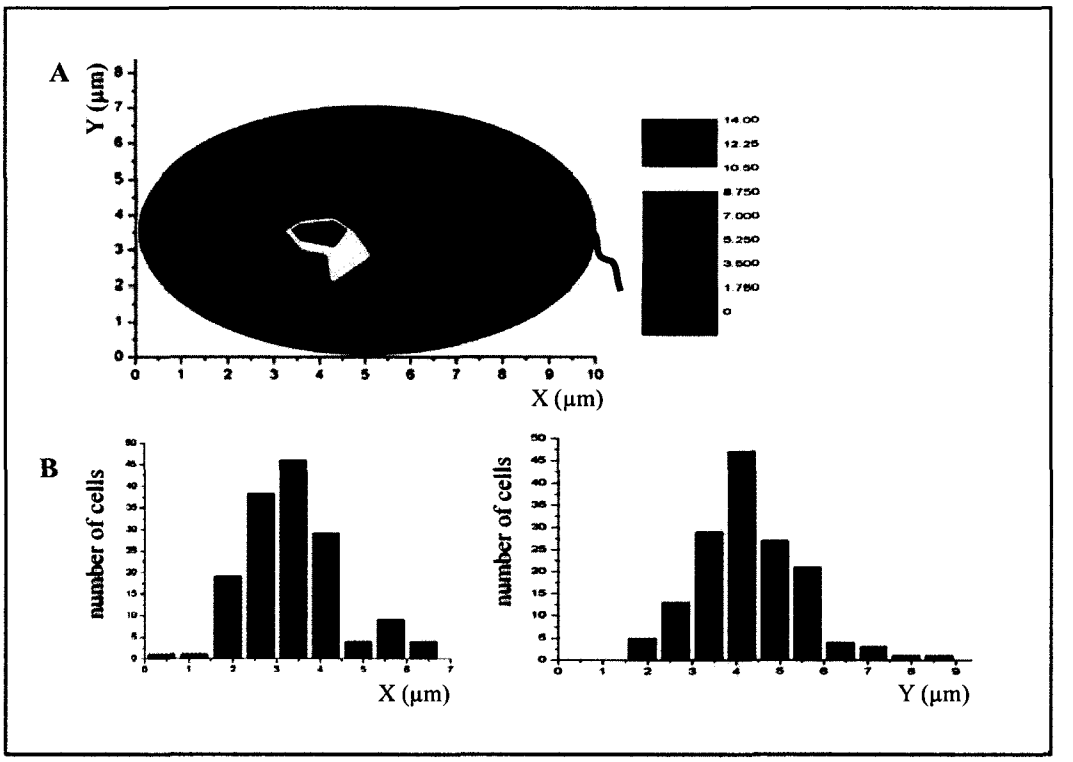

Figure 20 Intranuclear positioning of HSA 19 in human spermatozoa. (A) Plot of CT centers distribution showing probability values, red color-highest probability of finding CHR in this area. (B) Frequency distribution of CT centers longitude (x) and radial (y) localization.

show frequency distribution of CT centers either along the long (X) or along short (Y) nuclear axis of ellipsoid sperm nuclei. Histograms are just the different way of data representation. The X-histograms of two CHRs studied demonstrated a single peak for

each, suggesting a certain position of CTs along the nucleus length. Preferential location of HSA 19 is the anterior half of the sperm nucleus and of HSA 18 - the posterior half. Thus, in mature spermatozoa these chromosomes occupy different and the well-defined longitudinal positions. The Y-histograms for HSA 18 CTs (Fig. 19B) displayed two peaks with almost equal heights, suggesting the existence of two equiprobable positions. Naturally, these symmetrical localizations are well visible on contour plots for HSA 18. The Y-histograms for HSA 19 CTs (Fig. 20B) demonstrated a single peak. This corresponds to HSA 19 localization on or close to the L axis, signifying the central location, also clearly visible on contour plot (Fig. 20A).

DISCUSSION

A common way to localize CTs is to perform FISH analysis using CHR specific painting probes. The CHR painting probes produce relatively large hybridization signals even in sperm where CHR are compact resulting in difficulties in CTs mapping, which may be overcome by image analysis. The use of CHR-specific CEN probes to localize the CTs in sperm meets another difficulty - in mature sperm all CENs are clustered into the chromocenter within small nuclear volume (Zalenskaya & Zalensky 2004) whereas the rest of CTs are located elsewhere.

In this work, FISH was used with painting CHR probes to assess CT location in sperm. FISH experiments were followed by statistical analysis using Origin software, which is a new approach for purpose of CHR localization. Such an assessment resulting in graphical representations allows simultaneous ascertaining of both radial and longitude intranuclear positioning of CHRs. Two human chromosomes of similar size were studied - HSA 18 and HSA 19. HSA 18 CTs was preferentially located in the posterior half of the

nucleus and close to the nuclear periphery. In contrast, HSA 19 was located in the nuclear interior and closer to the acrosome. Importantly, clear differences in locations relative to the sperm nuclear membrane were established for CHRs different in gene numbers. Similar tendency in radial positioning of the gene rich CHR 19 (internal) and gene-poor CHR 18 (peripheral) has been demonstrated for somatic cells (Croft *et al.* 1999). Therefore, the proposed correlation between radial localization of CHRs and their gene density (Croft *et al.* 1999, Cremer *et al.* 2001) is preserved during spermatogenesis. CHR localization in sperm may participate in differential expression of male genome after fertilization.

Are sperm chromosomes distributed symmetrically with respect to long nuclear axis?

The contour plot for HSA 18 (Fig. 19) exhibits an interesting feature of CHR localization - a mirror symmetry with respect to nuclear ellipsoid long axis, that is, the two "halves" of the contour plot appeared as mirror-images of one another. There was no uniform lateral distribution of CT centers, which would be expected as a result of assumed rotational symmetry along L. Data for HSA 19 does not reflect such symmetry since this chromosome is located very close to the long axis. Similar observations were made by Gurevitch (Gurevitch *et al.* 2001) and Zalenskaya and Zalensky (Zalenskaya & Zalensky 2004) from their studies on CEN positioning in Hsp.

In conclusion, the observed symmetrical positioning seen here may arise as a result of two possible depositions of flattened sperm cells onto slide (flipping coin model). The flattened shape of Hsp cells was reported previously (Zalensky *et al.* 1995, Rens *et al.* 1999, Kovacs *et al.* 2008). The flat shape of spermatozoa remains preserved

after all steps of FISH routine, treatment with decondensing agents, denaturation, and exposure to ethanol (Zalensky *et al.* 1995).

CHAPTER VI

VISUALIZATON OF HUMAN SPERM CHROMOSOMES IN ZYGOTES

INTRODUCTION

By fertilization, two terminally differentiated cells, sperm and egg, are combined to create a totipotent zygote. The inactive sperm nucleus is being transformed in a coordinated fashion into a functional mPN within cytoplasm of an activated egg (Sutovsky & Schatten 2000). During the first hours (0-5 hr) post fertilization, paternal CHRs interact directly with ooplasm factors due to sperm nuclear envelope break down (Surani 2001). Very little is known about the mechanism of mPN formation and its movement towards the fPN. Assumed but mostly unexplored steps include sperm CHR withdrawal, replacement of PRMs with histones leading to chromatin decondensation, and paternal genome activation.

It is believed that transformations that take place in the developing mPN depend on the machinery provided by the ooplasm. The role of the sperm nuclear structures and molecular entities in this process is poorly understood. From the current knowledge of genome organization in sperm, it could be predicted that paternal CHRs are withdrawn in a certain order in space and time and that for each CHR there is a stepwise rather than simultaneous exposure of different domains to the ooplasm (Zalensky & Zalenskaya 2007). As a result, each chromatin domain is decondensed and remodeled at a certain time which provides differential gene activation patterns in the early embryo (Foster *et al.* 2005). In addition, specific longitude and radial positioning of each CHR in Hsp (Hazzouri *et al.* 2000, Zalenskaya & Zalensky 2004, Mudrak *et al.* 2005, Mandevelyan *et*

al. 2008, Chapter V) may participate in differential genome remodeling. We propose that CHRs that are closest to the nuclear edge and to the point of sperm primary contact with egg (subacrosomal region) should be exposed to ooplasm and remodeled first. To study this hypothesis, methods of sperm CHR visualization in the zygote should be developed. FISH with CHR-specific painting or CEN probes in application to embryos has been widely used to study aneuploidy. For such studies, preservation of nuclear or CHR topology is unimportant, therefore all protocols use a spread preparation of zygotes (Coonen *et al.* 1994, Harper *et al.* 1994) and then standard FISH with target objects fixed on slide. In the present study, a FISH protocol in solution was established that does not notably disrupt 3D organization and allows imaging of CHRs in zygotes. This approach was used to visualize unwinding of sperm CTs in the developing mPN.

MATERIALS AND METHODS

Preparation of sperm for ICSI

Preparation was performed exactly as described in Chapter III. Briefly, the cells were thoroughly washed from seminal fluid and the final sperm pellet was resuspended in mHTF–BSA. The plasma membranes from sperm cells were removed using 0.5% Triton X-100. Sperm was used for ICSI after extensive washings from detergent. In some experiments sperm tail was stained with MitoTracker.

Oocyte preparation and ICSI

For heterologous ICSI we used frozen HO from Conception Technologies (San Diego). Preparation of oocytes for injection has been described in Chapter III (Jones *et al.* 2010) and only viable oocytes (97%) were used.

ICSI was carried out according to (Palermo *et al.* 1992, Jones *et al.* 2010). Details of procedure have been described (Chapters II and III). Briefly, sperm suspension was diluted with 10% PVP and drop placed in the center of an injection dish. Each frozen-thawed mature (metaphase II) HO was placed in 5 µl drops surrounding sperm suspension, covered with mineral oil and injected using Narishige micromanipulator mounted on a phase-contrast inverted microscope. At least 30 metaphase II HO were microinjected for each experimental time (total n = 174 injected oocytes; at least 2 replicates for each time point). The injected oocytes were kept at 37°C in 5% CO_2 for 4, 8, 12 and 16 hr in P1 medium with 10% SSS. Incubation continued for specific time intervals and zygotes were withdrawn at indicated time points.

Fluorescent in situ hybridization

Zona pellucida was removed with Acid Tyrode's then zygotes were fixed in 2% paraformaldehyde for 45 min. Zygotes were stored in 0.2% Tween 20/PBS at 4°C for up to 2 weeks before performing hybridization. Whole chromosome painting probes for HSA 18 and 19 directly labeled with FITC and Rhodamine, respectively, were purchased from ID Labs, Inc. (London, Ontario, Canada). In a typical experiment, zygotes were permeabilized in 5% TX for 30 min at RT. Zygotes were then washed with 0.2% Tween 20/PBS for 5 min twice. Zygotes were dehydrated in 25, 50 and 100% methanol (MeOH)/0.2%Tween 20/PBS for two min each. Zygotes were then rehydrated by placing the zygotes through the MeOH series in reverse order for two min each. After rinsing in 0.2% Tween 20/PBS for 5 min, zygotes were placed in 20% formamide (FA)/0.2% Tween 20/PBS for 15 min at RT then transferred to 50% FA/Tween 20/PBS for 20 min. In the smallest volume possible, zygotes were then transferred in a microcentrifuge tube

containing concentrated painting probes (3 μl) and hybridization mixture (7 μl). Both probe and zygotes were denatured for 10 min at 75°C and then hybridized overnight at 37°C. Post hybridization washings were performed by placing zygotes in 50% FA/Tween 20/PBS for 30 min at RT. Zygotes were subsequently rinsed in 0.2% Tween 20/PBS for 10 min at RT prior to mounting using Vectashield containing DAPI or PI.

Microscopy and data analysis

The same procedures as described in Chapter III were used here. Briefly, hybridization results were visualized on Leitz Ortholux fluorescent microscope. Images were collected using a MagnaFire digital color camera and MicroFire software (Optronics). For each PN, four images were taken with selective and multi-band pass filters. Images were processed with Adobe Photoshop 7.0 software. Typically, about 162 mPN demonstrating similar structural elements were analyzed. Statistical analysis was performed in Microsoft Excel.

RESULTS

To visualize structural remodeling of sperm CHRs during mPN development in hybrid zygotes we performed "in-solution" FISH with HSA18 painting probe. Taking into consideration mPN heterogeneity established earlier (Chapters III and IV, Jones *et al.* 2010) stages of mPN development were roughly graded by NA size (see Chapter IV). At early stages of decondensation (~100 pixels^2), HSA 18 CT remained condensed and compact (Fig. 21, left panels). In more developed PN with size range >1000 pixels^2, the CT expanded and took up an unwound and relaxed configuration (Fig. 21, right panels). In most zygotes of this category, sperm CHRs demonstrated an extended shape with largely dispersed chromatin. Noticeably, several areas of condensed DNA remained,

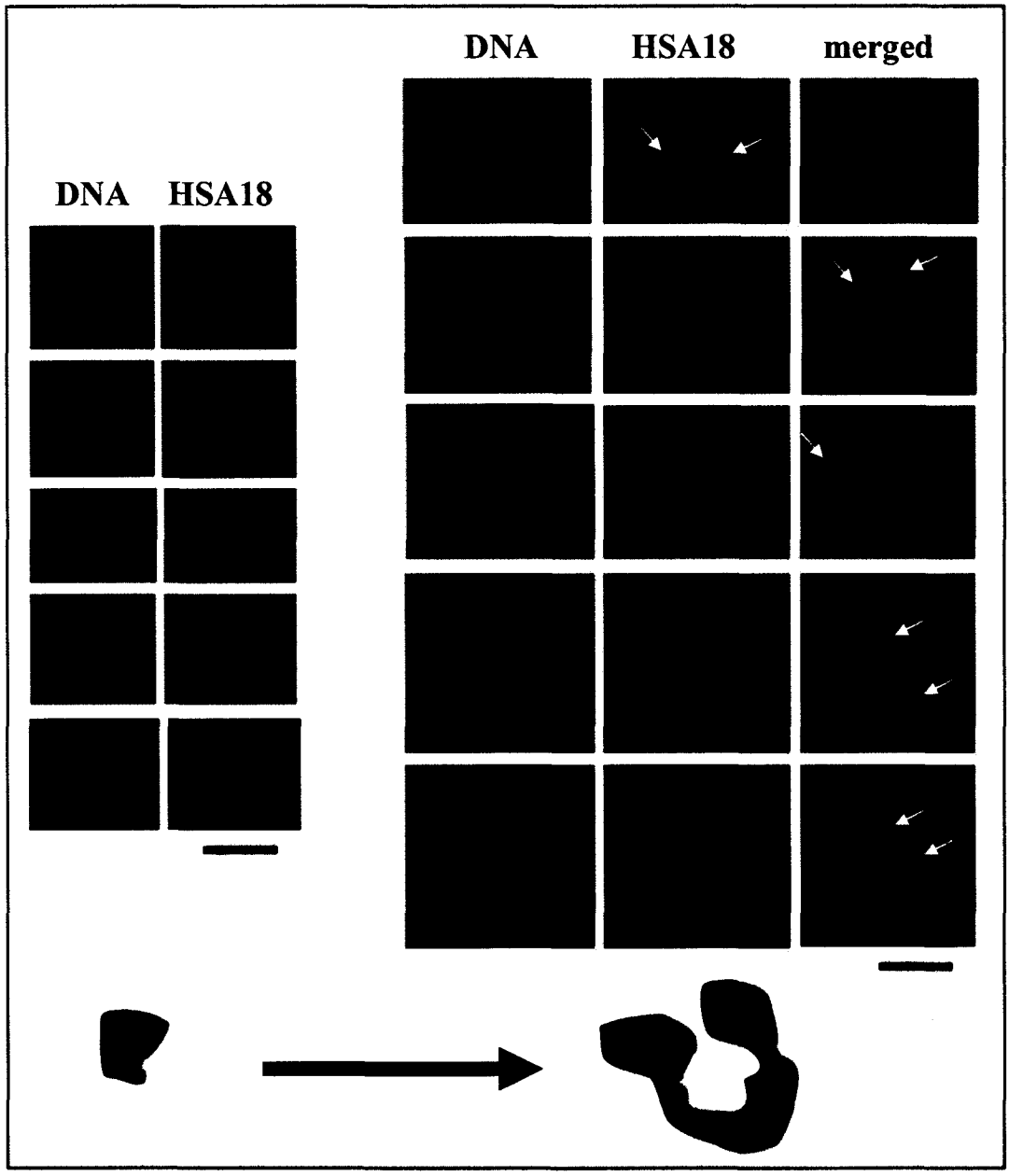

Figure 21 Unpacking of the sperm chromosome territory in zygotes produced from human sperm - hamster oocyte ICSI. Shown mPNs are enlarged cut-outs from whole zygote images. Left panels minimally decondensed PN, right panels - fully decondensed PN. Arrows indicate heterochromatic domains of CHR. FISH using HSA 18 painting probe (green), total DNA (blue). Scale bars 10 μm.

which most probably correspond to heterochromatic regions (Fig. 21, arrows). Data of Fig. 21 demonstrate feasibility of chromosome imaging in mPN that permits observation of structural changes in CT.

The long-term goal of this research is to establish relationship between CHR localization in sperm, extent of CT remodeling in developing PN and paternal genome activation. Such an objective demands the possibility of simultaneous imaging of two (and more) CHR in mPN. Here, HSA 18 and HSA 19 were localized using two-color

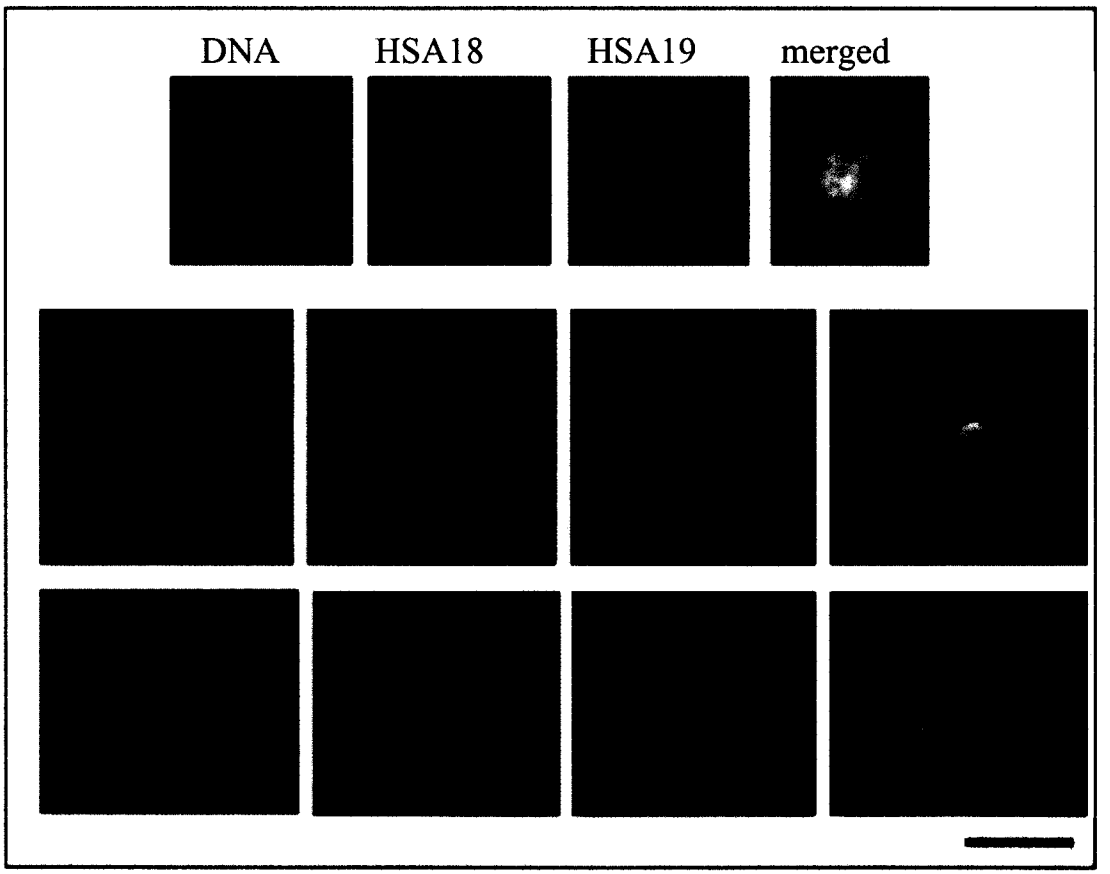

Figure 22 Simultaneous imaging of two human chromosomes in zygotes produced using human sperm - hamster oocyte ICSI. Shown mPNs are enlarged cut-outs from the whole zygote images. FISH using whole chromosome painting probes - HSA 18 (green), HSA 19 (red), total DNA (blue). Scale bar 10 μm.

FISH with painting probes labeled with different fluorochromes. Data presented on Fig. 22 demonstrate our capability to visualize two CTs. Hybridization signals produced by HSA 18 and HSA 19 were registered using selective filters which permit measurements and comparison of CTs size (area after 2D microscopy or volume after confocal microscopy) at different stages of mPN development.

DISCUSSION

According to the working hypothesis, non-random CHR positioning in sperm (Luetjens *et al.* 1999, Hazzouri *et al.* 2000; Zalenskaya & Zalensky 2004; Mudrak *et al.*, 2007; Chapter V) may determine sequential activation of paternal genome following fertilization. See Chapter V for a detailed discussion.

Initial approach to resolve this question is to establish if the differences in CHR remodeling during mPN development depend on their localization in sperm. Our previous work demonstrated that in sperm, gene-rich HSA 19 was positioned centrally while gene-poor HSA 18 - peripherally. To follow their localization and structural reorganization in mPN, a FISH "in-solution" protocol was set up and applied to hybrid human-hamster zygotes. Recently, FISH protocols that preserve structural organization of chromatin in early embryos have been developed (Koehler *et al.* 2009). This scheme while producing good results is extremely lengthy (more than a week). Our data (Fig. 21) demonstrate that quality FISH data may be obtained within 2 days.

A preliminary outline of Hsp CHR unfolding in PN developing in HO using FISH localization of HSA 18 was presented here. At the initial stages of decondensation, tight, compact CTs in the majority of cells (Fig. 21, left panels) were visualized. As NA increased, CTs adopted extended, unfolded configurations that were almost parallel to the

long nuclear axis (Fig. 21, right panels). In the process of nuclear decondensation, heterochromatic regions behaved differently from the rest of the CHR and maintained compact configurations (Fig. 21, arrows). Interestingly, overall behavior of sperm CHR in zygote was similar to that observed *in vitro* by FISH with arm-specific probes for HSA 1, HSA 2, and HSA 5 during artificial sperm decondensation with Heparin/DTT treatment (Mudrak *et al.* 2005).

Due to the variations in mPN size observed at each time point post ICSI (Chapters III and V), comparative kinetics of CHR processing may be studied only by simultaneous imaging of CHRs in one zygote. To this end, localization of HSA 18 and HSA 19 using two color FISH (Fig. 22) was optimized. This is an essential step for establishing if in the developing mPN peripherally localized HSA 18 will be decondensed earlier than HSA 19, positioned internally. Experiments in this direction are currently in progress.

In conclusion, some features of Hsp CHR transformation under the influence of ooplasm in a heterologous ICSI model were described in this work. We propose that the remodeling of the male gamete nuclei in this system mimics events that occur during natural human fertilization. At this point, this work is only preliminary and further studies are planned to strictly follow the sperm CHR transformation/processing in our heterologous ICSI model. We expect that this approach will be fruitful in understanding reorganization of the male genome at fertilization.

CHAPTER VII

SUMMARY

Due to the inability to conduct studies with human embryos, adequate model systems are necessary to study sperm chromatin transformation during the early events of fertilization. In preliminary studies, a noticeable relocalization of sperm CENs and remodeling of CTs were demonstrated using cell free extracts from *Xenopus Laevis* eggs. These results raised the possibility that unique genome architecture of sperm is reorganized in an ordered fashion during fertilization, the hypothesis of this dissertation.

This research focused on establishing an approach which we believe faithfully models early steps of natural fertilization in humans. The study focused on the introduction and application of heterologous ICSI to study sperm CHR remodeling. Two ICSI pairs (Hsp and bovine oocytes; Hsp and hamster oocytes) were explored in detail and the latter was chosen for further studies as robust and providing an apparently accurate model of the male gamete development.

The detailed kinetics of sperm chromatin decondensation within definite time intervals after ICSI was established. Several characteristics of Hsp remodeling were demonstrated: 1) sperm cells with partially destroyed membranes and depletion of the acrosome decondense more rapidly and to a greater extent than membrane/acrosome intact cells; 2) marked variability in mPN size was observed for all time points as detected by DNA staining in zygotes. We propose this characteristic reflects the cryptic heterogeneity in the mature, morphologically normal sperm population.

Next, the state of the chromatin/CHRs in developing mPN was characterized. Chromatin transformation was established by immunolocalizaton of PRMs in developing

zygotes. PRM withdrawal from human sperm nuclei was studied for the first time. In heterologous model used, the overall disappearance of PRMs from Hsp is rather rapid and most likely completed within 1 hr. Again, significant variation in mPN size from zygote to zygote was observed at any given time point studied. Importantly, it was demonstrated that PRM removal correlates with PN area rather than with time of Hsp exposure to hamster ooplasm. This supports the hypothesis of the importance of sperm population variability for dynamic (and perhaps success) of zygote development.

The final part of the investigation involved the study of two human chromosomes – HSA 18 and HSA 19. It was shown that in sperm: 1) both CHRs are packed into compact territories; and 2) similar to somatic cells, gene-rich HSA 19 is positioned internally while gene-poor HSA 18 peripherally. Thus, this feature of CHRs radial positioning according to gene density is preserved in terminally differentiated sperm cells. Subsequently, a FISH protocol was established for the visualization of human CHRs in zygotes. Gradual unwinding of compact chromosome territories of HSA 18 and HSA 19 was initially described. The observed mode of CHR unpacking resembles characteristic steps established earlier for sperm nuclei artificially swollen *in vitro* and may be encoded within specific sperm CHR architecture.

These findings demonstrate several novel aspects involving the dynamics of Hsp genome spatial reorganization during the process of mPN formation and development at fertilization. We propose that the remodeling of human male gamete nuclei during heterologous ICSI faithfully mimics major steps that occur during natural fertilization.

Thus, the heterologous ICSI approach explored here appears to be a valuable way to study different aspects of human male genome remodeling during fertilization. Still

elusive molecular factors and mechanisms responsible for PRM removal, nuclear decondensation and CHR remodeling may be studied using available modern techniques of single-cell analysis. Importantly, the developed approaches may be used in basic research intended to improve existing ART techniques and understand some fertilization failures. As direct human experiments are not possible, the use of abnormally fertilized triploid embryos or oocytes which had fertilization failure from human ICSI of consenting patients could be analyzed to characterize some of the same points illustrated by the heterologous model, i.e. retention of the acrosome, PRM removal and CHR positioning.

REFERENCES

Adenot PG, Mercier Y, Renard JP & Thompson EM 1997 Differential H4 acetylation of paternal and maternal chromatin precedes DNA replication and differential transcriptional activity in pronuclei of 1-cell mouse embryos. *Development* **124** 4615-4625.

Ahmadi A & Ng SC 1997 Fertilization and development of mouse oocytes injected with membrane-damaged spermatozoa. *Human Reproduction* **12** 2797-2801.

Ahmadi A & Ng SC 1997 Sperm head decondensation, pronuclear formation, cleavage and embryonic development following intracytoplasmic sperm injection of mitochondria-damaged sperm in mammals. *Zygote* **5** 247-253.

Ahmadi A & Ng SC 1999 Destruction of protamine in human sperm inhibits sperm binding and penetration in the zona-free hamster penetration test but increases sperm head decondensation and male pronuclear formation in the hamster-ICSI assay. *Journal of Assisted Reproduction and Genetics* **16** 128-132.

Aiken RJ 1984 Diagnostic value of the hamster oocyte penetration assay. *International Journal of Andrology* **7** 273-275.

Ajduk A, Yamauchi Y & Ward MA 2006 Sperm chromatin remodeling after intracytoplasmic sperm injection differs from that of in vitro fertilization. *Biology of Reproduction* **75** 442-451.

Aoki VW, Emery BR & Carrell DT 2006 Global sperm deoxyribonucleic acid methylation is unaffected in protamine-deficient infertile males. *Fertility and Sterility* **86** 1541-1543.

Arpanahi A, Brinkworth M, Iles D, Krawetz SA, Paradowska A, Platts AE, Saida M, Steger K, Tedder P & Miller D 2009 Endonuclease-sensitive regions of human spermatozoal chromatin are highly enriched in promoter and CTCF binding sequences. *Genome Research* **19** 1338-1349.

Balhorn R 2007 The protamine family of sperm nuclear proteins. *Genome Biology* **8** 227.

Balhorn R, Cosman M, Thornton K, Krishnan VV, Corzett M, Bench G, Kramer C, Lee J, Hud NV, Allen M & et.al. 1999 Protamine-mediated condensation of DNA in mammalian sperm. In: The Male Gamete: from Basic Knowledge to Clinical Applications, pp. 55-70. Ed C Gagnon Vienna, IL: Cache River Press.

Banerjee S, Smallwood A & Hulten M 1995 ATP dependent reorganization of human sperm nuclear chromatin. *Journal of Cell Science* **108** 755-765.

Bedford JM & Calvin HI 1974 The occurrence and possible functional significance of -S-S-crosslinks in sperm heads, with particular reference to eutherian mammals. *Journal of Experimental Zoology* **188** 137-156.

Bench AJ, Nacheva EP, Champion KM & Green AR 1998 Molecular genetics and cytogenetics of myeloproliferative disorders *Baillieres Clinical Haematology* **11** 819-848.

Bonduelle M, Liebaers I, Derde MP, Camus M, Devroey P & Van Steirtegham A 2002 Neonatal data on a cohort of 2889 infants born after ICSI (1991-1999) and of 2995 infants born after IVF (1983-1999). *Human Reproduction* **17** 671-694.

Braun RE 2001 Packaging paternal chromosomes with protamine. *Nature Genetics* **28** 10-12.

Brown DB, Blake EJ, Wolgemuth DJ, Gordon K & Ruddle FH 1987 Chromatin decondensation and DNA synthesis in human sperm activated in vitro by using *Xenopus laevis* egg extracts. *Journal of Experimental Zoology* **242** 215-231.

Burns KH, Viveiros MM, Ren Y, Wang P, DeMayo FJ, Frail DE, Eppig JJ & Matzuk MM 2003 Roles of NPM2 in chromatin and nucleolar organization in oocytes and embryos. *Science* **300** 633-636.

Calvin HI & Bedford JM 1971 Formation of disulfide bonds in the nucleus and accessory structures of mammalian spermatozoa during maturation in the epididymis. *Journal of Reproduction and Fertility* Supplement **13** 65-75.

Chen SH & Seidel Jr GE 1997 Effects of oocyte activation and treatment of spermatozoa on embryonic development following intracytoplasmic sperm injection in cattle. *Theriogenology* **48** 1265-1273.

Cho C, Willis WD, Goulding EH, Jung-Ha H, Choi YC, Hecht NB & Eddy EM 2001 Haploinsufficiency of protamine-1 or -2 causes infertility in mice. *Nature Genetics* **28** 82-86.

Chung JT, Keefer CL & Downey RB 2000 Activation of bovine oocytes following intracytoplasmic sperm injection (ICSI). *Theriogenology* **53** 1273-1284.

Claussen U 2005 Chromosomics. *Cytogenetic and Genome Research* **111** 101-106.

Collas P & Poccia D 1998 Remodeling the sperm nucleus into a male pronucleus at fertilization. *Theriogenology* **49** 67-81.

Coonen E, Dumoulin JC, Ramaekers FC & Hopman AH 1994 Optimal preparation of preimplantation embryo interphase nuclei for analysis by fluorescence in-situ hybridization. *Human Reproduction* **9** 533-537.

Cremer T & Cremer C 2001 Chromosome territories, nuclear architecture and gene regulation in mammalian cells. *Nature Reviews. Genetics* **2** 292-301.

Cremer T, Kurz A, Zirbel R, Dietzel S, Rinke B, Schrock E, Speicher MR, Mathieu U, Jauch A, Emmerich P & et al. 1993 Role of chromosome territories in the functional compartmentalization of the cell nucleus. *Cold Spring Harbor Symposia on Quantitative Biology* **58** 777-792.

Cremer T, Kupper K, Dietzel S & Fakan S 2004 Higher order chromatin architecture in the cell nucleus: on the way from structure to function. *Biology of the Cell* **96** 555-567.

Croft JA, Bridger JM, Boyle S, Perry P, Teague P & Bickmore WA 1999 Differences in the localization and morphology of chromosomes in the human nucleus. *Journal of Cell Biology* **145** 1119-1131.

Dehghani H, Dellaire G & Bazett-Jones DP 2005 Organization of chromatin in the interphase mammalian cell. *Micron* **36** 95-108.

Dernburg AF & Sedat JW 2005 Mapping three-dimensional chromosome architecture in situ. *Methods in Cell Biology* **53** 187-233.

de Yebra L, Ballesca JL, Vaniell JA, Bassas L & Oliva R 1993 Complete selective absence of protamine P2 in humans. *The Journal of Biological Chemistry* **268** 10553-10557.

Ecklund PS & Levine L 1975 Mouse sperm basic nuclear protein electrophoretic characterization and fate after fertilization. *Journal of Cell Biology* **66** 251-262.

Evenson DP & Wixon R 2005 Comparison of the Halosperm test kit with sperm chromatin structure assay (SCSA) infertility test in relation to patient diagnosis and prognosis. *Fertility and Sterility* **84** 846-849.

Fazeli A, Hage WJ, Cheng FP, Voorhout WF, Mark SA, Bevers MM & Colenbrander B 1997 Acrosome-intact boar spermatozoa initiate binding to the homologous zona pellucida *in vitro*. *Biology of Reproduction* **56** 430-438.

Fedorova E & Zink D 2009 Nuclear genome organization: common themes and individual patterns. *Current Opinion in Genetics and Development* **19** 166-171.

Finch KA, Fonseka KG, Abogrein A, Ioannou D, Handyside AH, Thornhill AR, Hickson N & Griffin DK 2008 Nuclear organization in human sperm: preliminary evidence for altered sex chromosome centromere position in infertile males. *Human Reproduction* **23** 1263-1270.

Foster HA, Abeydeera LR, Griffin DL & Bridger JM 2005 Non-random chromosome positioning in mammalian sperm nuclei with migration of the sex chromosomes during late spermatogenesis. *Journal of Cell Science* **118** 1811-1820.

Foster HA & Bridger JM 2005 The genome and the nucleus: a marriage made by evolution. Genome organization and nuclear architecture. *Chromosoma* **114** 212-229.
Fraser P & Bickmore W 2007 Nuclear organization of the genome and the potential for gene regulation. *Nature* **447** 413-417.

Frehlick LJ, Eirin-Lopez JM & Ausio J 2007 New insights into the nucleophosmin/nucleoplasmin family of nuclear chaperones. *Bioessays* **29** 49-59.

Fulka H, Mrazek M, Tepla O & Fulka J Jr 2004 DNA methylation pattern in human zygotes and developing embryos. *Reproduction.* **128** 703-708.

Fulka H, Barnetova I, Mosko T & Fulka J 2008 Epigenetic analysis of human spermatozoa after injection into ovulated mouse oocytes. *Human Reproduction* **23** 627-634.

Fung J, Weier Hu & Pederson RA 2001 Detection of structural and numerical chromosome abnormalities in interphase cells using spectral imaging. The *Journal of Histochemistry and Cytochemistry* **49** 797-798.

Gerlich D, Beaudouin J, Kalbfuss B, Daigle N, Eils R & Ellenburg J 2003 Global chromosome positions are transmitted through mitosis in mammalian cells. *Cell* **112** 751-761.

Gilbert N, Gilchrist S & Bickmore WA 2005 Chromatin organization in the mammalian nucleus. *International Review of Cytology* **242** 283-336.

Gotto K, Kinoshita A, Takuma Y & Ogawa K 1990 Fertilization of bovine oocytes by the injection of immobilized, killed sperm. *The Veterinary Record* **24** 517-520.

Goud PT, Goud AP, Rybouccbkin AV, DeSutter P & Dhont M 1998 Chromatin decondensation, pronucleus formation, metaphase entry and chromosome complements of human spermatozoa after intracytoplasmic sperm injection into hamster oocytes. *Human Reproduction* **13** 1336-1345.

Govin J, Caron C, Lestrat C, Rousseaux S & Khochbin S 2004 The role of istones in chromatin remodeling during mammalian spermiogenesis. *European Journal of Biochemistry* **271** 3459-3469.

Greaves IK, Rens W, Ferguson-Smith MA, Griffin D & Marshall Graves JA 2003 Conservation of chromosome arrangement and position of the X in mammalian sperm suggests functional significance. *Chromosome Research* **11** 503-512.

Gurevitch M, Amiel A, Ben-Zion M, Fejgin M & Bartoov B 2001 Acrocentric centromere organization within the chromocenter of the human sperm nucleus. *Molecular Reproduction and Development* **60** 507-516.

Haaf T & Ward DC 1995 Higher order nuclear structure in mammalian sperm revealed by in situ hybridization and extended chromatin fibers. *Experimental Cell Research* **219** 604-611.

Hagstrom KA & Meyer BJ 2003 Condensin and cohesin: more than chromosome compactor and glue. *Nature Reviews. Genetics* **4** 520-534.

Hamano K, Li X, Funauchi K, Furudate M & Minato Y 1999 Gender preselection in cattle with intracytoplasmically injected, flow cytometrically sorted sperm heads. *Biology of Reproduction* **60** 1194-1197.

Hammoud SS, Purwar J, Pflueger C, Cairns BR & Carrell DT 2009 Alterations in sperm DNA methylation patterns at imprinted loci in two classes of infertility. *Fertility and Sterility* (article in press).

Harper JC, Robinson F, Duffy S, Griffin DK, Handyside AH, Delhanty JD & Winston RM 1994 Detection of fertilization in embryos with accelerated cleavage by fluorescent in-situ hybridization (FISH). *Human Reproduction* **9** 1733-1737.

Hazzouri M, Rousseaux S, Mongelard F, Usson Y, Pelletier R, Faure AK, Vourc'h C & Sele B 2000 Genome organization in the human sperm nucleus studied by FISH and confocal microscopy. *Molecular Reproduction and Development 55* 307–315.

Hershlag A, Kaplan EH, Loy RA, DeCherney AH & Lavy G 1992 Selection bias in in vitro fertilization programs. *American Journal of Obstetrics and Gynecology* **166** 1-3.

Hewitson L, Dominko T, Takahashi D, Martinovich D, Neuringer M, Battagli D, Simerly C & Schatten G 1999 Unique checkpoints during the first cell cycle of fertilization after intracytoplasmic sperm injection in rhesus monkeys. *Nature Medicine* **5** 431-433.

Hewitson, L, Haavisto, L, Simerly, C, Jones, J & Schatten, G 1997 Microtubule Organization and chromatin donfigurations in hamster oocytes during fertilization and parthenogenetic activation, and after insemination with human sperm. *Biology of Reproduction 57* 967-975.

Horiuchi T, Emuta C, Yamauchi Y, Oikawa T, Numabe T & Yanagimachi R 2002 Birth of normal calves after intracytoplasmic sperm injection of bovine oocytes: a methodological approach. *Theriogenology* **57** 1013-1024.

Foster HA, Abeydeera LR, Griffin DL & Bridger JM 2005 Non-random chromosome positioning in mammalian sperm nuclei with migration of the sex chromosomes during late spermatogenesis. *Journal of Cell Science* **118** 1811-1820.

Foster HA & Bridger JM 2005 The genome and the nucleus: a marriage made by evolution. Genome organization and nuclear architecture. *Chromosoma* **114** 212-229.
Fraser P & Bickmore W 2007 Nuclear organization of the genome and the potential for gene regulation. *Nature* **447** 413-417.

Frehlick LJ, Eirin-Lopez JM & Ausio J 2007 New insights into the nucleophosmin/nucleoplasmin family of nuclear chaperones. *Bioessays* **29** 49-59.

Fulka H, Mrazek M, Tepla O & Fulka J Jr 2004 DNA methylation pattern in human zygotes and developing embryos. *Reproduction.* **128** 703-708.

Fulka H, Barnetova I, Mosko T & Fulka J 2008 Epigenetic analysis of human spermatozoa after injection into ovulated mouse oocytes. *Human Reproduction* **23** 627-634.

Fung J, Weier Hu & Pederson RA 2001 Detection of structural and numerical chromosome abnormalities in interphase cells using spectral imaging. The *Journal of Histochemistry and Cytochemistry* **49** 797-798.

Gerlich D, Beaudouin J, Kalbfuss B, Daigle N, Eils R & Ellenburg J 2003 Global chromosome positions are transmitted through mitosis in mammalian cells. *Cell* **112** 751-761.

Gilbert N, Gilchrist S & Bickmore WA 2005 Chromatin organization in the mammalian nucleus. *International Review of Cytology* **242** 283-336.

Gotto K, Kinoshita A, Takuma Y & Ogawa K 1990 Fertilization of bovine oocytes by the injection of immobilized, killed sperm. *The Veterinary Record* **24** 517-520.

Goud PT, Goud AP, Rybouccbkin AV, DeSutter P & Dhont M 1998 Chromatin decondensation, pronucleus formation, metaphase entry and chromosome complements of human spermatozoa after intracytoplasmic sperm injection into hamster oocytes. *Human Reproduction* **13** 1336-1345.

Govin J, Caron C, Lestrat C, Rousseaux S & Khochbin S 2004 The role of istones in chromatin remodeling during mammalian spermiogenesis. *European Journal of Biochemistry* **271** 3459-3469.

Greaves IK, Rens W, Ferguson-Smith MA, Griffin D & Marshall Graves JA 2003 Conservation of chromosome arrangement and position of the X in mammalian sperm suggests functional significance. *Chromosome Research* **11** 503-512.

Kikuchi K, Nakai M, Shimada A & Kashiwazaki N 2006 Production of viable porcine embryos by in vitro fertilization (IVF) and intracytoplasmic sperm injection (ICSI). *Journal of Mammalian Ovary Research* **23** 96-106.

Kim NH, Jun SH, Do JT, Uhm SJ, Lee HT & Chung KS 1999 Intracytoplasmic sperm injection of porcine, bovine, mouse, or human spermatozoa into porcine oocytes. *Molecular Reproduction and Development* **53** 84-91.

Kimura Y & Yanagimachi R 1995 Intracytoplasmic sperm injection in the mouse. *Biology of Reproduction* **52** 709-720.

Koehler D, Zakhartchenko V, Froenicke L, Stone G, Stanyon R, Wolf E, Cremer T & Brero A 2009 Changes of higher order chromatin arrangements during major genome activation in bovine preimplantation embryos. *Experimental Cell Research* **315** 2053-2063.

Kopecny V & Pavlok A 1975 Incorporation of Arginine-3H into chromatin of mouse eggs shortly after sperm penetration. *Histochemistry* **45** 341-345.

Kovacs T, Bekesi G, Fabian A, Rakosy Z, Harvath G, Matyus L, Balazs M & Jenei A 2008 DNA flow cytometry of human spermatozoa: consistent stoichiometric staining of sperm DNA using a novel decondensation protocol. *Cytometry* **73** 965-970.

Lee JD, Kamiguchi Y & Yanagimachi R 1996 Analysis of chromosome constitution of human spermatozoa with normal and aberrant head morphologies after injection into mouse oocytes. *Human Reproduction* **11** 1942-1946.

Lewis JD, Song Y, de Jong ME, Bagha SM & Ausio J 2003 A walk through vertebrate and invertebrate protamines. *Chromosoma* **111** 473-482.

Liu CT, Chen CH, Cheng SP & Ju JC 2002 Parthenogenesis of rabbit oocytes activated by different stimuli. *Animal Reproduction Science* **70** 267-276.

Lohka MJ & Masui Y 1983 Formation in vitro of sperm pronuclei and mitotic chromosomes induced by amphibian ooplasmic components. *Science* **220** 719-721.

Luetjens CM, Payne C & Schatten G 1999 Non-random chromosome positioning in human sperm and sex chromosome anomalies following intracytoplasmic sperm injection. *Lancet* **353** 1240.

Manvelyan M, Hunstig F, Bhatt S, Mrasek K, Pellestor F, Weise A, Simonyan I, Aroutiounian R & Liehr T 2008 Chromosome distribution in human sperm- a 3D multicolor banding-study. *Molecular Cytogenetics* **14** 1-25.

Martianov I, Brancorsini S, Gansmuller A, Parvinen M, Davidson I & Sassone-Corsi P 2002 Distinct functions of TBP and TLF/TRF2 during spematogenesis:

requirement of TLF for heterochromatic chromocenter formation in haploid round spermatids. *Development* **129** 945-955.

McFadden DE & Friedman JM 1997 Chromosome abnormalities in human beings. *Mutation Research* **396** 129-140.

McLay DW & Clarke HJ 2003 Remodeling the paternal chromatin at fertilization in mammals. *Reproduction* **125** 625-33.

Mehta IS, Elcock LS, Amira M, Kill IR & Bridger JM 2008 Nuclear motors and nuclear structures containing A-type lamins and emerin: is there a functional link? *Biochemical Society Transactions* **36** 1384-1388.

Meistrich ML, Brock WA, Grimes SR, Platz RD & Hnilica LS 1978 Nuclear protein transitions during spermatogenesis. *Federation Proceedings* **37** 2522-2525.

Meistrich ML, Mohapatra B, Shirley CR & Zhao M 2003 Roles of transition nuclear proteins in spermiogenesis. *Chromosoma* **111** 483-488.

Meo SC, Yamazaki W, Ferreira CR, Perecin F & Saraiva NZ 2007 Parthenogenetic activation of bovine oocytes using single and combined strontium, ionomycin and 6-dimethylaminopurine treatments. *Zygote* **15** 295-306.

Meyer-Ficca M, Muller-Navia J & Scherthan H 1998 Clustering of pericentromeres initiates in step 9 of spermiogenesis of the rat (Rattus norvegicus) and contributes to a well defined genome architecture in the sperm nucleus. *Journal of Cell Science* **111** 1363-1370.

Misteli T 2004 Spatial positioning: a new dimension in genome function. *Cell* **119** 153-156.

Montag M Tok V, Liow SL. Bongso A & Ng SC 1992 In vitro decondensation of mammalian sperm and subsequent formation of pronuclei-like structures for micromanipulation. *Molecular Reproduction and Development* **33** 338-346.

Morozumi K & Yanagimachi R 2005 Incorporation of the acrosome into the oocyte during intracytoplasmic sperm injection could be potentially hazardous to embryo development. *Proceedings of the National Academy of Sciences of the United States of America* **102** 14209-14214.

Mudrak O, Tomilin N, & Zalensky A 2005 Chromosome Architecture in the Decondensing Human Sperm Nucleus. *Journal of Cell Science* **118** 4541-4550.

Mudrak OS, Tomilin NV & Zalensky AO 2007 Decompactization of chromosome 1 in the artificially decondensed human sperm nuclei: overall topology and non-random location of chromosome bends. *Tsitologiia* **49** 149-155.

Mudrak O, Chandra R, Jones E, Godfrey E, & Zalensky A 2009 Reorganization of human sperm nuclear architecture during formation of pronuclei in a model system. *Reproduction, Fertility and Development* 21 665-671.

Nakamura S, Terada Y, Horiuchi T, Emuta C, Murakami T, Yaegashi N & Okamura K 2001 Human sperm aster formation and pronuclear decondensation in bovine eggs following intracytoplasmic sperm injection using piezo-driven pipette: a novel assay for human sperm centrosomal function. *Biology of Reproduction* **65** 1359-1363.

Nakazawa Y, Shimada A, Noguchi J, Domeki I, Kaneko H & Kikuchi K 2002 Replacement of nuclear protein by histone in pig sperm nuclei during in vitro fertilization. *Reproduction* **124** 565-572.

Nazarov IB, Shlyakhtenko LS, Lyubchendo YL, Zalenskaya IA & Zalensky AO 2008 Sperm chromatin released by nucleases. *Systems Biology in Reproductive Medicine* **54** 37-46.

Neuber E, Havari E, Aquiles Sanchez J, Powers RD & Wangh LJ 1999 Efficient human sperm pronucleus formation and replication in *Xenopus* egg extracts. *Biology of Reproduction* **61** 912-920.

Nonchev S & Tsanev R 1990 Protamine-histone replacement and DNA replication in the male mouse pronucleus. *Molecular Reproduction and Development* **25** 72-76.

Ohsumi K, Katagiri C & Yanagimachi R 1988 Human sperm nuclei can transform into condensed chromosomes in *Xenopus* egg extracts. *Gamete Research* **20** 1-9.

Oliva R 2006 Protamines and male infertility. *Human Reproduction Update* **12** 417-435.

Palermo G, Joris H, Devroey P & Van Steirteghem AC 1992 Pregnancies after intracytoplasmic injection of single spermatozoon into an oocyte. *Lancet* **340** 17-18.

Parada LA, McQueen PG & Misteli T 2004 Tissue-specific spatial organization of genomes. *Genome Biology* **5** R44.

Perreault SD 1992 Chromatin remodeling in mammalian zygotes. *Mutation* Research **296** 43-55.

Perreault SD, Barbee RP, Elstein KH, Zucker RM & Keefer CL 1988 Interspecies differences in the stability of mammalian sperm nuclei assessed in vivo by sperm microinjection and in vitro by flow cytometry. *Biology of Reproduction* **8** 1061-1066.

Poccia D & Collas P 1996 Transforming sperm nuclei into male pronuclei in vivo and in vitro. *Current Topics in Developmental Biology* **34** 25-88.

Ramirez MJ & Surralles J 2008 Laser confocal microscopy analysis of human interphase nuclei by three-dimensional FISH reveals dynamic perinucleolar clustering of telomeres. *Cytogenetics and Genome Research* **122** 237-242.

Rens W, Welch GR & Johnson L 1999 Improved flow cytometric sorting of X- and Y-chromosome bearing sperm: substantial increase in yield of sexed semen. *Molecular Reproduction and Development* **52** 50-56.

Rho GJ, Kawarsky S, Johnson WH, Kochhar K & Betteridge KJ 1998 Sperm and oocyte treatments to improve the formation of male and female pronuclei and subsequent development following intracytoplasmic sperm injection into bovine oocytes. *Biology of Reproduction* **59** 918-924.

Rodman TC, Pruslin FH, Hoffmann HP & Alfrey VG 1981 Turnover of basic chromosomal proteins in fertilized eggs: a cytoimmunochemical study of events in vivo. *Journal of Cell Biology* **90** 351-361.

Romano R, Santucci R, Marrone V, Gabriele AR, Necozione S, Valenti M, Francavilla S & Francavilla F 1998 A prospective analysis of the accuracy of the Test-yolk buffer enhanced hamster egg penetration test and acrosin activity in discriminating fertile from infertile males. *Human Reproduction* **13** 2115-2121.

Rogers BJ, Perreault SD, Brentwood BJ, McCarville C, Hale R & Soderdahl DW 1983 Variability in human-hamster in vitro assay for fertility evaluation. *Fertility and Sterility* **39** 204-211.

Sakkas D, Urner F, Bizzaro D, Manicardi G, Bianchi PG, Shoukir Y & Campana A 1998 Sperm nuclear DNA damage and altered chromatin structure: effect on fertilization and embryo development. *Human Reproduction* **13** 11-19.

Sathananthan AH, Tatham B, Dharmawardena V, Grills B, Lewis I & Trounson A 1997 Inheritance of sperm centrioles and centrosomes in bovine embryos. *Archives of Andrology* **38** 37-48.

Sbracia M, Baldi M, Cao D, Sandrelli A, Chiandetti A, Poverini R & Aragona C 2002 Preferential location of sex chromosomes, their aneuploidy in human sperm, and their role in determining sex chromosome aneuploidy in embryos after ICSI. *Human Reproduction* **17** 320-324.

Schatten G, Simerly C & Schatten H 1991 Maternal inheritance of centrosomes in mammals? Studies of parthenogenetic and polyspermy in mice. *Proceedings of the National Academy of Science USA* **88** 6785-6789.

Scherthan H, Weich S, Schwegler H, Heyting C, Harle M & Cremer T 1996 Centromere and telomere movements during early meiotic prophase of mouse and man

are associated with the onset of chromosome pairing. *Journal of Cell Biology* **134** 1109-1125.

Schmid TE, Brinkworth MH, Hill F, Sloter E, Kamischke A, Marchetti F, Nieschlag E & Wyrobek AJ 2004 Detection of structural and numerical chromosomal abnormalities by ACM-FISH analysis in sperm of oligozoospermic infertility patients. *Human Reproduction* **19** 1395-1400.

Schultz RM & Worrad DM 1995 Role of chromatin structure in zygotic gene activation in the mammalian embryo. *Seminars in Cell Biology* **6** 201-208.

Schwartz D, Ducot B, Auroux M & Collin C 1986 Variability of the percentage of morphologically abnormal spermatozoa: biological and measurement components. *Human Reproduction* **1** 369-371.

Seita Y, Junya ITO & Kashiwazaki N 2009 Removal of acrosomal membrane from sperm head improves development of rat zygotes derived from intracytoplasmic sperm injection. *Journal of Reproduction and Development* (in press).

Shi Q & Martin RH 2001 Aneuploidy in human spermatozoa: FISH analysis in men with constitutional chromosomal abnormalities and in infertile men. *Reproduction* **211** 655-666.

Shimada A, Kikuchi K, Noguchi J, Akama K, Nakamo M & Kaneko H 2000 Protamine dissociation before decondensation of sperm nuclei during in vitro fertilization of pig oocytes. *Journal of* Reproduction **120** 247-256.

Singleton S, Mudrak O, Morshedi M, Oehninger S, Zalenskaya I & Zalensky A 2007 Characterization of a human sperm cell subpopulation marked by the presence of the TSH2B histone. *Reproduction, Fertility and Development* **19** 392-397.

Singleton S, Zalensky A, Doncel GF, Morshedi M & Zalenskaya IA 2007 Testis/sperm-specific histone 2B in the sperm donors and subfertile patients: variability and relation to chromatin packaging. *Human Reproduction* **22** 743-750.

Sloter ED, Lowe X, Mode II DH, Nath J & Wyrobek AJ 2000 Multicolor FISH analysis of chromosomal breaks, duplications, deletions, and numerical abnormalities in sperm of healthy men. *American Journal of Human Genetics* **67** 862-872.

Sloter E, Nath J, Eskenazi B & Wyrobek AJ 2004 Effects of male age on the frequencies of germinal and heritable chromosomal abnormalities in humans and rodents. *Fertility and Sterility* **81** 925-943.

Solovei IV, Joffe BI, Hori T, Thomson P, Mizumo S & Macgregor HC 1998 Unordered arrangement of chromosomes in the nuclei of chicken spermatozoa. *Chromosoma* **107** 184-188.

Solov'eva L, Svetiova M, Bodinski D & Zalensky AO 2004 Nature of telomere dimmers and chromosome looping in human spermatozoa. *Chromosome Research* **12** 817-823.

Spector DK 2003 The dynamics of chromosome organization and gene regulation. *Annual Review of Biochemistry* **72** 573-608.

Stricker SA 1999 Comparative biology of calcium signaling during fertilization and egg activation in animals. *Developmental Biology* **211** 157-176.

Surani MA 2001 Reprogramming of genome function through epigenetic inheritance. *Nature* **414** 122-128.

Sutovsky P, Hewisotn L, Simerly CR, Tengowski MW, Navara CS, Hasvisto A & Schatten G 1996 Intracytoplasmic sperm injection for Rhesus monkey fertilization results in unusual chromatin, cytoskeletal, and membrane events, but eventually leads to pronuclear development and sperm aster assembly. *Human Reproduction* **11** 1703-1712.

Sutovsky P & Schatten G 1997 Depletion of glutathione during bovine oocyte maturation reversibly blocks the decondensation of the male pronucleus and pronuclear apposition during fertlisation. *Biology of Reproduction* **56** 1503-1512.

Sutovsky, P & Schatten, G 2000 Paternal contributions to the mammalian zygote: fertilization after sperm-egg fusion. *International Review of Cytology* **195** 1-65.

Suttner R, Zakhartchenko V, Stojkovitc P, Muller S, Alberio R, Medjugorac I, Brem G, Wolf E & Stojkovic M 2000 Intracytoplasmic sperm injection in bovine: effects of oocyte activation, sperm pre-treatment and injection technique. *Theriogenology* **54** 935-948.

Tanemura K, Ogura A, Cheong C, Gotoh H, Matsumoto K, Sato E, Hayashi Y, Lee HN & Kondo T 2005 Dynamic rearrangement of telomeres during spermatogenesis in mice. *Developmental Biology* **281** 196-207.

Tanphaichitr N, Sobhon P, Taluppeth N & Chalermisarachai P 1978 Basic nuclear proteins in testicular cells and ejaculated spermatozoa in man. *Experimental Cell Research* **117** 347-356.

Tateno H & Kamiguchi Y 1999 Dithiothreitol induces sperm nuclear decondensation and protects against chromosome damage during male pronuclear formation in hybrid zygotes between Chinese hamster spermatozoa and Syrian hamster oocytes. *Zygote* **7** 321-327.

Tempest HG & Griffin DK 2004 The relationship between male infertility and increased levels of sperm disomy. *Cytogenetic and Genome Research* **107** 83-94.

Terada Y, Luetjens CM, Sutovsky P & Schatten G 2000 Atypical decondensation of the sperm nucleus, delayed replication of the male genome, and sex chromosome positioning following intracytoplasmic human sperm injection (ICSI) into golden hamster eggs: does ICSI itself introduce chromosomal anomalies? *Fertility and Sterility* **74** 454-460.

Terada Y 2004 Human sperm centrosome function during fertilization, a novel assessment for male sterility. *Human Cell* **17** 181-186.

Terada Y, Hasegawa H, Takahashi A, Ugaijn T, Yaegashi N & Okamura K 2009 Successful pregnancy after oocyte activation by a calcium ionophore for a patient with recurrent intracytoplasmic sperm injection failure, with an assessment of oocyte activation and sperm centrosomal function using bovine eggs. *Fertility and Sterility* **91** 935.

Thomson I, Gilchrist S, Bickmore WA & Chubb JR 2004 The radial positioning of chromatin is not inherited through mitosis but is established de novo in early G1. *Current Biology* **14** 166-172.

Tilgen, N, Guttenbach, M & Schmid, M 2001 Heterochromatin is not an adequate explanation for close proximity of interphase chromosomes 1–Y, 9–Y, and 16–Y in human spermatozoa. *Experimental Cell Research* **265** 283-287.

Uehara T & Yanagimachi R 1976 Micorsurgical injection of spermatozoa inoto eggs with subsequent transformation of sperm nuclei into male pronuclei. *Biology of Reproduction* **15** 467-470.

Van Roijen, JH, Ooms, MP, Spaargaren MC, Baarends WM, Weber RFA, Grootegoed JA & Vreeburg JT 1998 Immunoexpression of testis-specific histone 2B in human spermatozoa and testis tissue. *Human Reproduction* **13** 1559-1566.

Van Steirteghem A, Nagy Z, Joris H, Liu J, Staessen C, Smitz J, Wisant A & Deveroey P 1993 High fertilization and implantation rates after intracytoplasmic sperm injection. *Human Reproduction* **8** 1061-1066.

van der Heijden GW, Dieker JW, Derijck AA, Muller S, Berden JHM, Braat D, van der Vlag J & de Boer P 2005 Asymmetry in histone H3 variants and lysine methylation between paternal and maternal chromatin of the early mouse zygote. *Mechanisms of Development* **122**1008-1022.

Van Steirteghem A, Bonduelle M, Devroey P & Liebaers I 2002 Follow up of children born after ICSI. *Human Reproduction* **8** 111-116.

Verschure PJ 2004 Positioning the genome within the nucleus. *Biology of the Cell* **96** 569-577.

Villenponteau B 1992 Heparin increases chromatin accessibility by binding the trypsin-sensitive basic residues in histones. *The Biochemical Journal* **288** 953-958.

Walter J, Schermelleh L, Cremer M, Tashiro S & Cremer T 2003 Chromosome order in HeLa cells changes during mitosis and G1m but is stably maintained during subsequent interphase stages. ***Journal of Cell Biology*** **160** 685-697.

Ward MA & Ward WS 2004 A model for the function of sperm DNA degradation. *Reproduction Fertility and Development* **16** 547-554.

Ward WS 2010 Function of sperm chromatin structural elements in fertilization and development. *Molecular Human Reproduction* **16** 30-36.

Ward WS & Coffey DS 1991 DNA packaging and organization in mammalian spermatozoa: Comparison with somatic cells. *Biology of Reproduction* **44** 569-574.

Wei H & Fukui Y 1999 Effects of bull, sperm type and sperm pre-treatment on male pronuclear formation after intracytoplasmic sperm injection in cattle. *Reproduction Fertility and Development* **11** 59-65.

Wiland E, Zegalo M & Kupisz M 2008 Interindividual differences and alterations in the topology of chromosomes in human sperm nuclei of fertile donors and carriers of reciprocal translocations. *Chromosome Research* **16** 291-305.

Williams RR & Fisher AG 2003 Chromosomes, positions please! *Nature Cell Biology* **5** 388-390.

World Health Organization (WHO) 1992 Laboratory manual for the examination of human semen and sperm-cervical mucus interaction edn 3. Cambridge: Cambridge University Press.

Wouters-Tyrou D, Martinage A, Chevaillier P & Sautiere P 1998 Nuclear basic proteins in spermiogenesis. *Biochimie* **80** 117-128.

Wright SJ & Longo FJ 1988 Sperm nuclear enlargement in fertilized hamster eggs is related to meiotic maturation of the maternal chromatin. *Journal of Experimental Zoology* **247** 155-165.

Wyrobek AJ, Schmid TE & Marchetti F 2005 Cross-species sperm-FISH assays for chemical testing and assessing paternal risk for chromosomally abnormal pregnancies. *Environmental and Molecular Mutagenesis* **45** 271-283.

Yamauchi Y, Yanagimachi R & Horiuchi T 2002 Full-term development of golden hamster oocytes following intracytoplasmic sperm head injection. Biology *of Reproduction* **67** 534-539.

Yanagida K, Yanagimachi R, Perreault SD & Kleinfeld RG 1991 Thermostability of sperm nuclei assessed by microinjection into hamster oocytes. *Biology of Reproduction* **44** 440-447.

Yanagimachi R, Yanagimachi H & Rogers BJ 1976 The use of zona free animal ova as a test system for the assessment of the fertilizing capacity of human spermatozoa. *Biology of Reproduction* **15** 471-476.

Yanagimachi R 1994 Mammalian fertilization. In the Physiology of Reproduction, edn 2, pp 189-317. Eds E Knobil and JD Neill New York: Raven Press.

Yanagimachi R 2005 Intracytoplasmic injection of spermatozoa and spermatogenic cells: its biology and applications in human and animals. *Reproductive Biomedicine* Online **10** 247-288.

Yoshimoto-Kakoi T, Terada Y, Tachibana M, Murakami T, Yaegashi N & Okamura K 2008 Assessing centrosomal function of infertile males using heterologous ICSI. *Systems Biology in Reproductive Medicine* **54** 135-142.

Zalenskaya IA, Bradbury EM & Zalensky AO 2000 Chromatin structure of telomere domain in human sperm. *Biochemical and Biophysical Research Communications* **279** 213-218.

Zalenskaya IA & Zalensky AO 2002 Telomeres in mammalian male germline cells. *International Review of Cytology* **218** 37-67.

Zalenskaya, IA & Zalensky, AO 2004 Non-Random positioning of chromosomes in human sperm nuclei. *Chromosome Research* **12** 1-11.

Zalensky AO, Breneman JW, Zalenskaya IA, Brinkly BR & Bradbury EM 1993 Organization of centromeres in the decondensed nuclei of mature human sperm. *Chromosoma* **102** 509-518.

Zalensky AO, Allen MJ, Kobayashi A, Zalenskaya IA, Balhorn R & Bradbury EM 1995 Well-defined genome architecture in the human sperm nucleus. *Chromosoma* **103** 577-590.

Zalensky AO, Tomilin NV, Zalenskaya IA, Teplitz RL & Bradbury EM 1997 Telomere-telomere interactions and candidate telomere binding protein(s) in mammalian sperm cells. *Experimental Cell Research* **232** 29-41.

Zalensky AO, Siino JS, Gineitis AA, Zalenskaya IA, Tomilin NV, Yau P, & Bradbury EM 2002 Human testis/sperm specific histone H2B (hTSH2B); Molecular cloning and characterization. *Journal of Biological Chemistry* **277** 43 474-43 480.

Zalensky A & Zalenskaya I 2007 Organization of chromosomes in spermatozoa: an additional layer of epigenetic information? *Biochemical Society transactions* **35** 609-611.

VITA

Estella Jones

Education:

2010	Ph.D. in Biomedical Sciences Eastern Virginia Medical School and Old Dominion University Department of Obstetrics and Gynecology, EVMS, Norfolk, VA
1999	M.S. in Biomedical Sciences Eastern Virginia Medical School, Norfolk, VA
1992	B.A. in Psychology and Biology Virginia Wesleyan College, Norfolk, VA

Publications, (*) included in dissertation:

Avendano C, Franchi A, **Jones E** & Oehninger S 2009 Pregnancy-specific {beta}-1 glycoprotein 1 and human leukocyte antigen-E mRNA I human sperm: differential expression in fertile and infertile men and evidence of a possible functional role during early development. *Human Reproduction* **24** 270-277.

Jones EL, Boyd CA, Dowling-Lacey D, Wright D, Mayer JF & Lanzendorf SE 2001 Evaluation of the meiotic spindle apparatus in metaphase II human oocytes following cytoplasmic donation. *Journal of Assisted Reproduction and Genetics* **18** 230-234.

(*) **Jones E**, Mudrak O & Zalensky A 2010 Kinetics of human male pronuclear development in a heterologous ICSI model. *Journal of Assisted Reproduction and Genetics* **27** 277-283.

(*) **Jones EL**, Zalensky AO, Zalenskaya IA 2010 Protamine withdrawal from human sperm nuclei following heterologous ICSI into hamster oocytes. *Protein and Peptide Letters* in press.

(*) Mudrak O, Chandra R, **Jones E**, Godfrey E & Zalensky A 2009 Reorganization of human sperm nuclear architecture during formation of pronuclei in a model system. *Reproduction, Fertility and Development* **21** 665-671.

(*) Mudrak O, **Jones E**, Nazarov I & Zalensky A 2010 Longitude positioning of chromosome territories in human spermatozoa is determined by centromere localization within linear arrays, in preparation for submission to *Journal of Cell Biology*.

Riggs R, Mayer J, Dowling-Lacey D, Chi TF, **Jones E** & Oehninger S 2010 Does storage time influence postthaw survival and pregnancy outcome? An analysis of 11,768 cryopreserved human embryos. *Fertility and Sterility* **93** 109-115.